energies

Article

Power Optimization of a Modified Closed Binary Brayton Cycle with Two Isothermal Heating Processes and Coupled to Variable-Temperature Reservoirs

Chenqi Tang [1,2,3], Lingen Chen [1,2,*], Huijun Feng [1,2], Wenhua Wang [3], Yanlin Ge [1,2]

1 Institute of Thermal Science and Power Engineering, Wuhan Institute of Technology, Wuhan 430205, China; tangchenqi7@163.com (C.T.); huijunfeng@139.com (H.F.); geyali9@hotmail.com (Y.G.)
2 School of Mechanical and Electrical Engineering, Wuhan Institute of Technology, Wuhan 430205, China
3 College of Power Engineering, Naval University of Engineering, Wuhan 430033, China; wwh_gt371@163.com
* Correspondence: lgchenna@yahoo.com or lingenchen@hotmail.com

Received: 27 May 2020; Accepted: 18 June 2020; Published: 20 June 2020

Abstract: A modified closed binary Brayton cycle model with variable isothermal pressure drop ratios is established by using finite time thermodynamics in this paper. A topping cycle, a bottoming cycle, two isothermal heating processes and variable-temperature reservoirs are included in the new model. The topping cycle is composed of a compressor, a regular combustion chamber, a converging combustion chamber, a turbine and a precooler. The bottoming cycle is composed of a compressor, an ordinary regenerator, an isothermal regenerator, a turbine and a precooler. The heat conductance distributions among the six heat exchangers are optimized with dimensionless power output as optimization objective. The results show that the double maximum dimensionless power output increases first and then tends to be unchanged while the inlet temperature ratios of the regular combustion chamber and the converging combustion chamber increase. There also exist optimal thermal capacitance rate matchings among the working fluid and heat reservoirs, leading to the optimal maximum dimensionless power output.

Keywords: finite time thermodynamics; modified binary Brayton cycle power plant; power output; energy saving; heat exchanger optimization

1. Introduction

Due to the characteristics of high power density (PD), small vibration, high automation, low operating pressure and easy lubrication, gas turbine plants (Brayton heat engine cycle) are extensively applied in the fields of aviation, energy, transportation, etc. According to the different working fluid (WF) circulation modes, the Brayton cycle is divided into open and closed cycles, and many works concerning the classical thermodynamic analyses and optimizations for various Brayton cycles have been performed [1–3]. The WF of closed Brayton cycle is not directly connected with the atmosphere, and does not participate in the combustion process. Hence, it is applied to convert nuclear energy, geothermal energy, solid fuel and other primary energy into electricity energy.

For the case of simple heating, the temperature of the gas elevates in the direction of a duct when the subsonic compressible gas flows through the smooth heating duct with a fixed cross-sectional area. For the case of simple cross-sectional area change, the temperature drops when the gas flows through the smooth adiabatic duct with a reduced cross-sectional area. Based on these two gas properties, the isothermal processes can be realized when the subsonic compressible gas flows through the smooth heating duct with a reduced cross-sectional area. Vecchiarelli et al. [4] presented a combustion chamber where the WF could be heated isothermally. The introduction of this type of combustion chamber could effectively improve the thermal efficiency (TEF) of the Brayton cycle, and reduce the emissions of nitrogen oxides and other harmful gases. Göktun and Yavuz [5] applied the isothermal heating combustion chamber to the regenerative Brayton cycle, and discovered the isothermal pressure drop ratio impacted the cycle performance significantly. Based on [5], Erbay et al. [6] compared the optimal performances of an isothermal heating regenerative Brayton cycle under maximum power output (PO) and maximum PD. Jubeh [7] found the exergy efficiency was enhanced by adding the isothermal heating combustion chamber in regenerative Brayton cycle. El-Maksoud [8] combined the isothermal concept and double Brayton cycle to establish a new cycle model. Based on [8], Qi et al. [9] derived the specific work and exergy efficiency, and analyzed the impacts of different parameters on the exergy efficiency. All those works were carried out by using classical thermodynamics.

Finite time thermodynamics (FTT) [10] have been extensively applied in the analyses and optimizations of many thermodynamic systems. The purpose of FTT is to reduce the irreversibilities of processes and cycles and to improve the energy utilization rates [11]. Plenty of FTT studies have been conducted for various heat engine cycles, including the Novikov engine [12], the Stirling engine [13], Rankine cycles [14–21], heated gas expansion process [22], thermoelectric generators [23–26], the fuel cell hybrid cycle [27], the gas–mercury combined cycle [28], the thermocapacitive heat engine [29], the Maisotsenko–Diesel cycle [30], the trigeneration cycle [31], Dual-Miller cycles [32–34], Feynman's ratchet [35], the Kalina cycle [36] and so on.

For the Brayton cycles, FTT studies have been also conducted for simple cycles [37], regenerative cycles [38–40], multi-intercooling-and-regenerative cycles [41–43], the fuel cell–Brayton combined cycle [44], Maisotsenko–Brayton cycles [45,46], Brayton cycle-based cooling, heat and power combined cycles [47,48] and so on.

For the Brayton cycles with isothermal heating modification, Kaushik et al. [49] optimized the regenerative Brayton cycle with isothermal process whose optimization objective was the PO. Tyagi et al. [50–56] optimized the performances of the isothermal heating modified simple, regenerated and intercooling Brayton cycles with different optimization objectives. Based on [49–56], Wang et al. [57,58] and Tang et al. [59,60] analyzed and optimized the endoreversible simple, irreversible simple and irreversible regenerative Brayton cycles with isothermal processes. Arora et al. [61] optimized the regenerative Brayton cycle with isothermal process by employing the NSGA-II algorithm.

Based on El-Maksoud's classical thermodynamic model [8], Qi et al. [62] established a closed endoreversible binary Brayton cycle model with two isothermal processes, without internal irreversibility, and coupled to constant-temperature reservoirs (CTRs). They derived the functional expressions of PO, TEF, PD and ecological function, respectively. The impacts of different thermodynamic parameters on the relationships among performance indexes and the pressure ratio of the topping cycle were analyzed, and the heat conductance distributions (HCDs) among heat exchangers were further optimized.

Based on the previously established cycle models in [8,62], a modified closed binary Brayton cycle (MCBBC) with variable isothermal pressure drop ratios and internal and external irreversibilities will be established by using FTT in this paper. The HCDs will be optimized with dimensionless PO. The influences of different thermodynamic parameters on the optimal performance will be analyzed, and the thermal capacitance rate matchings (TCRMs) among the WF and the heat reservoirs will be also discussed.

2. Cycle Model

Figure 1a shows the schematic diagram of the MCBBC with two isothermal heating processes [8]. A topping cycle and a bottoming cycle are included in the model. The topping cycle is composed of a compressor (Com1), a regular combustion chamber (RCC), a converging combustion chamber (CCC), a turbine (Tur1) and a precooler (PC1). The bottoming cycle is composed of a compressor (Com2), an ordinary regenerator (OR), an isothermal regenerator (IR), a turbine (Tur2) and a precooler (PC2).

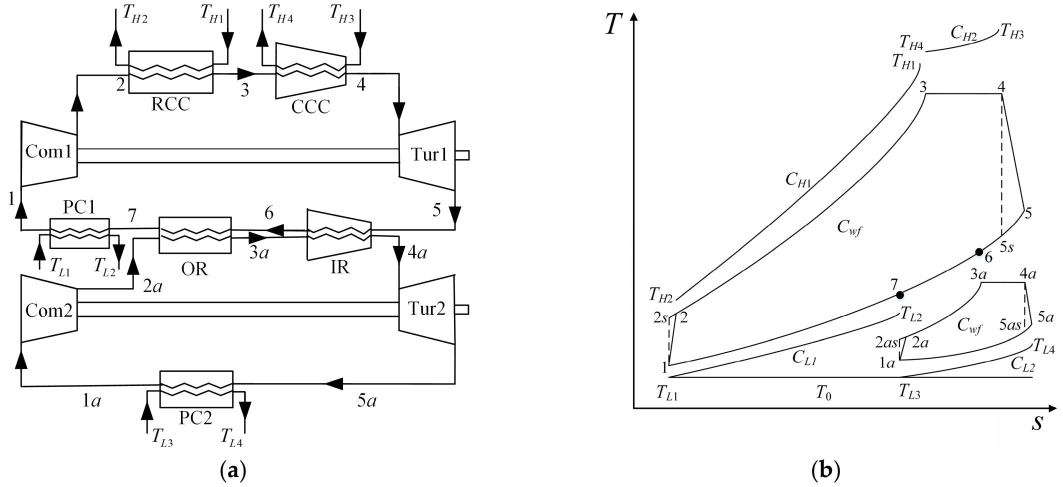

Figure 1. (**a**) Schematic diagram of the cycle [8]; (**b**) *T*-*s* diagram of the cycle.

Figure 1b illustrates the *T*-*s* diagram of the MCBBC. In the figure, processes $1 \to 2$, $2 \to 3$, $3 \to 4$, $4 \to 5$, $5 \to 6$, $6 \to 7$ and $7 \to 1$ represent the irreversible adiabatic compression, isobaric heating, isothermal heating, irreversible adiabatic expansion and three isobaric exothermic processes of the WF in Com1, RCC, CCC, Tur1, IR, OR and PC1, respectively. Processes $1a \to 2a$, $2a \to 3a$, $3a \to 4a$, $4a \to 5a$ and $5a \to 1a$ represent the irreversible adiabatic compression, isobaric heating, isothermal heating, irreversible adiabatic expansion and isobaric exothermic process of the WF in Com2, OR, IR, Tur2 and PC2, respectively. Processes $1 \to 2s$, $4 \to 5s$, $1a \to 2as$ and $4a \to 5as$ are the isentropic processes corresponding to the processes $1 \to 2$, $4 \to 5$, $1a \to 2a$ and $4a \to 5a$ respectively.

It is assumed that the WFs of the topping and bottoming cycles are the same, both of which are ideal gases. The specific heat at constant pressure, thermal capacity rate, specific heat ratio, mass flow rate and gas constant of the WF are C_p, C_{wf}, k, $\dot{m}$ and R_g, respectively, where $C_{wf} = C_p \dot{m}$ and $m = (k-1)/k$. The temperatures and pressures at different state points are signed as T_i and P_i ($i = 1,2,3,4,5,6,7,1a,2a,3a,4a,5a,2s,5s,2as,5as$), and the ambient temperature is T_0. The inlet temperatures of the outer fluids in the RCC, CCC, PC1 and PC2 are T_{H1}, T_{H3}, T_{L1} and T_{L3}, and the outlet temperatures of outer fluids in the RCC, CCC, PC and PC2 are T_{H2}, T_{H4}, T_{L2} and T_{L4}, respectively. The thermal capacity rates of outer fluids in the RCC, CCC, PC1 and PC2 are C_{H1}, C_{H2}, C_{L1} and C_{L2}, respectively. The pressure ratios in the Com1 and Com2 are π_{com1} and π_{com2}, and the isothermal pressure drop ratios at the CCC and IR are π_t and π_{ta}, respectively. The heat conductances of the heat exchangers for the RCC, CCC, OR, IR, PC1 and PC2 are U_j ($j = H1, H2, R1, R2, L1, L2$), and the corresponding effectivenesses are E_j; namely:

$$E_{H1} = \frac{1 - \exp[-N_{H1}(1 - C_{H1min} / C_{H1max})]}{1 - (C_{H1min} / C_{H1max}) \exp[-N_{H1}(C_{H1min} / C_{H1max})]} \tag{1}$$

$$E_{H2} = 1 - \exp(-N_{H2}),\ E_{R1} = N_{R1} / (N_{R1} + 1),\ E_{R2} = 1 - \exp(-N_{R2}) \tag{2}$$

$$E_{L1} = \frac{1 - \exp[-N_{L1}(1 - C_{L1min} / C_{L1max})]}{1 - (C_{L1min} / C_{L1max}) \exp[-N_{L1}(C_{L1min} / C_{L1max})]} \tag{3}$$

$$E_{L2} = \frac{1 - \exp[-N_{L2}(1 - C_{L2min} / C_{L2max})]}{1 - (C_{L2min} / C_{L2max})\exp[-N_{L2}(C_{L2min} / C_{L2max})]} \tag{4}$$

where $C_{H1max} = max\{C_{wf}, C_{H1}\}$, $C_{H1min} = min\{C_{wf}, C_{H1}\}$, $C_{L1max} = max\{C_{wf}, C_{L1}\}$, $C_{L1min} = min\{C_{wf}, C_{L1}\}$, $C_{L2max} = max\{C_{wf}, C_{L2}\}$ and $C_{L2min} = min\{C_{wf}, C_{L2}\}$. The numbers of heat transfer units for the heat exchangers are calculated as:

$$N_{H1} = U_{H1} / C_{H1min}, N_{H2} = U_{H2} / C_{H2} \tag{5}$$

$$N_{R1} = U_{R1} / C_{wf}, N_{R2} = U_{R2} / C_{wf} \tag{6}$$

$$N_{L1} = U_{L1} / C_{L1min}, N_{L2} = U_{L2} / C_{L2min} \tag{7}$$

When $C_{H1max} = C_{H1min}$, $C_{L1max} = C_{L1min}$ and $C_{L2max} = C_{L2min}$, Equations (1), (3) and (4) are simplified into:

$$E_{H1} = N_{H1} / (N_{H1} + 1), E_{L1} = N_{L1} / (N_{L1} + 1), E_{L2} = N_{L2} / (N_{L2} + 1) \tag{8}$$

The efficiencies in the Com1, Com2, Tur1 and Tur2 are η_{com1}, η_{com2}, η_{tur1} and η_{tur2}, respectively:

$$\eta_{\text{com1}} = (T_{2s} - T_1) / (T_2 - T_1) \tag{9}$$

$$\eta_{\text{com2}} = (T_{2as} - T_{1a}) / (T_{2a} - T_{1a}) \tag{10}$$

$$\eta_{\text{tur1}} = (T_4 - T_5) / (T_4 - T_{5s}) \tag{11}$$

$$\eta_{\text{tur2}} = (T_{4a} - T_{5a}) / (T_{4a} - T_{5as}) \tag{12}$$

The heat absorbing rates of WF in the RCC, CCC, OR and IR are $\dot{Q}_{2-3}$, $\dot{Q}_{3-4}$, $\dot{Q}_{2a-3a}$ and $\dot{Q}_{3a-4a}$, and the heat releasing rates in the PC1 and PC2 are $\dot{Q}_{7-1}$ and $\dot{Q}_{5a-1a}$. They are calculated as:

$$\dot{Q}_{2-3} = C_{H1}(T_{H1} - T_{H2}) = C_{wf}(T_3 - T_2) = C_{Hmin}E_{H1}(T_{H1} - T_2) \tag{13}$$

$$\dot{Q}_{3-4} = C_{H2}(T_{H3} - T_{H4}) = C_{H2}E_{H2}(T_{H3} - T_3) = \dot{m}(V_4^2 - V_3^2) / 2 \tag{14}$$

$$\dot{Q}_{2a-3a} = C_{wf}(T_{3a} - T_{2a}) = C_{wf}(T_6 - T_{H2}) = C_{wf}E_{R1}(T_6 - T_{2a}) \tag{15}$$

$$\dot{Q}_{3a-4a} = C_{wf}(T_5 - T_6) = C_{wf}E_{R2}(T_5 - T_{3a}) = \dot{m}(V_{4a}^2 - V_{3a}^2) / 2 \tag{16}$$

$$\dot{Q}_{7-1} = C_{wf}(T_7 - T_1) = C_{L1}(T_{L2} - T_{L1}) = C_{L1min}E_{L1}(T_7 - T_{L1}) \tag{17}$$

$$\dot{Q}_{5a-1a} = C_{wf}(T_{5a} - T_{1a}) = C_{L2}(T_{L4} - T_{L3}) = C_{L2min}E_{L2}(T_{5a} - T_{L3}) \tag{18}$$

The power output and thermal efficiency of the cycle are W and η, respectively:

$$W = \dot{Q}_{2-3} + \dot{Q}_{3-4} - \dot{Q}_{5a-1a} - \dot{Q}_{7-1} \tag{19}$$

$$\eta = W / (\dot{Q}_{2-3} + \dot{Q}_{3-4}) \tag{20}$$

Processes 3–4 and 3a–4a are the isothermal ones, and the heat absorbing rates of the two processes are:

$$\dot{Q}_{3-4} = \dot{m}(h_4 - h_3) - \dot{m}\int_3^4 v dp = \dot{m}R_g T_3 \ln \pi_t \tag{21}$$

$$\dot{Q}_{3a-4a} = \dot{m}(h_{4a} - h_{3a}) - \dot{m}\int_{3a}^{4a} v dp = \dot{m}R_g T_{3a} \ln \pi_{ta} \tag{22}$$

Processes 1–2s, 1–2as, 4–5s and 4a–5as are the isentropic processes; namely:

$$T_{2s} / T_1 = \pi_{\text{com1}}^m = x, T_{2as} / T_{1a} = \pi_{\text{com2}}^m = x_a \tag{23}$$

$$T_4/T_5 = \pi_{\text{com1}}^m \pi_t^m = xy, T_{4a}/T_{5a} = \pi_{\text{com2}}^m \pi_{ta}^m = x_a y_a \tag{24}$$

where x, y, x_a and y_a are the parameters of temperature ratios which can be calculated by the pressure ratios.

The upper limits of π_t and π_{ta} are 1, which means that the isothermal heating is not used. When $\pi_t < 1$ or $\pi_{ta} < 1$, the topping or bottoming cycle adopts the isothermal process. The isothermal pressure drop ratios must meet the following constraints:

$$\pi_t \geq \pi_{\text{com1}}^{-1}, \pi_{ta} \geq \pi_{\text{com2}}^{-1} \tag{25}$$

$$\ln \pi_t = \frac{-C_p(k-1)(M_4^2 - M_3^2)}{2R_g} = -0.7(M_4^2 - M_3^2) \tag{26}$$

$$\ln \pi_{ta} = \frac{-C_p(k-1)(M_{4a}^2 - M_{3a}^2)}{2R_g} = -0.7(M_{4a}^2 - M_{3a}^2) \tag{27}$$

where M_3 and M_4 (M_{3a} and M_{4a}) are the Mach numbers at the inlet and outlet of CCC (IR), respectively. If $M_3 = M_{3a} = 0$ and $M_4 = M_{4a} = 1$, $(M_4^2 - M_3^2)$ and $(M_{4a}^2 - M_{3a}^2)$ get their maximum values of 1, and π_t and π_{ta} get their minimum values of 0.4966. For the initial velocity of the WF, the Mach numbers satisfy $M_3 = M_{3a} = 0.2$ and $M_4 = M_{4a} = 1$, and the corresponding minimum values of π_t and π_{ta} are 0.5107. At the same time, $\bar{W}$ must be greater than or equal to zero; otherwise, the cycle is meaningless.

The major difference between the model in this paper and that in [8] is that all the heat transfer losses in the six heat exchangers are considered in this paper. This is also the major difference between classical thermodynamic model and FTT model. The major differences between the model in this paper and that in [62] are two aspects: One is that the irreversible compression and expansion losses are considered in this paper; this is also the major difference between the endoreversible model and the irreversible one. Another is that the heat reservoirs are assumed to be variable-temperature ones in this paper; this is one of basic characteristics of practical closed engineering cycles.

According to the above model, the dimensionless PO $\bar{W}$ and TEF η can be given by:

$$\bar{W} = \frac{\begin{array}{c}\{a_1 a_2 + T_{H3} - C_{H1min} E_{H1}(a_1 a_2 + T_{H1})/C_{wf}\} C_{H2} E_{H2} + C_{H1min} E_{H1}(a_1 a + T_{H1}) \\ + C_{wf}(a_4 - a_5) - C_{wf}[a_1 a_2 \eta_{\text{com1}}/(\eta_{\text{com1}} + x - 1) + a_3]\end{array}}{C_{wf} T_0} \tag{28}$$

$$\eta = 1 - \frac{C_{wf}[(a_1 a_2 \eta_{\text{com1}})/(\eta_{\text{com1}} + x - 1) + a_3 - a_4 + a_5]}{C_{H2} E_{H2}\{-C_{H1min} E_{H1}(a_1 a_2 + T_{H1})/C_{wf} + a_1 a_2 + T_{H3}\} + C_{H1min} E_{H1}(a_1 a_2 + T_{H1})} \tag{29}$$

where a_1, a_2, a_3, a_4 and a_5 are listed in Appendix A.

If Equations (21) and (22) are not considered when solving Equations (28) and (29), the final analytical solutions for $\bar{W}$ and η of the cycle cannot be obtained. Considering Equations (21) and (22), the values of x and y in Equations (28) and (29) are obtained by numerical calculation, and the corresponding values of $\bar{W}$ and η can be obtained.

If C_{H1}, C_{H2}, C_{L1}, C_{L2}, E_{H1}, E_{H2}, E_{R1}, E_{R2}, E_{L1}, E_{L2}, η_{com1}, η_{com2}, η_{tur1} and η_{tur2} take different values, the model can be converted into different special models; Equations (28) and (29) can be reduced to the corresponding dimensionless PO and TEF respectively, which have a certain universality.

When $\eta_{\text{com1}} = \eta_{\text{com2}} = \eta_{\text{tur1}} = \eta_{\text{tur2}} = 1$, Equations (28) and (29) can be reduced to the dimensionless PO and TEF of a modified closed endoreversible binary Brayton cycle with two isothermal heating processes and coupled to variable-temperature heat reservoirs (VTHRs):

$$\bar{W} = \frac{C_{H2}E_{H2}\{b_1b_2 + T_{H3} - C_{H1min}E_{H1}(b_1b_2 + T_{H1}) / C_{wf}\} - C_{wf}[b_1b_2 / x + b_3] + C_{H1min}E_{H1}(b_1b_2 + T_{H1}) + C_{wf}(b_4 - b_5)}{C_{wf}T_0} \tag{30}$$

$$\eta = 1 - \frac{C_{wf}[b_1b_2 / x + b_3 - b_4 + b_5]}{C_{H2}E_{H2}\{b_1b_2 + T_{H3} - [C_{H1min}E_{H1}(b_1b_2 + T_{H1})] / C_{wf}\} + C_{H1min}E_{H1}(b_1b_2 + T_{H1})} \tag{31}$$

where b_1, b_2, b_3, b_4 and b_5 are listed in Appendix A.

When $C_{H1} = C_{H2} = C_{L1} = C_{L2} \to \infty$, Equations (28) and (29) can be reduced to the dimensionless PO and TEF of a modified closed irreversible binary Brayton cycle with two isothermal heating processes and coupled to CTRs:

$$\bar{W} = \frac{C_{H2}E_{H2}[c_1c_2 + T_{H3} - E_{H1}(c_1c_2 + T_{H1})] - C_{wf}[c_1c_2\eta_{\text{com1}} / (\eta_{\text{com1}} + x - 1) + c_3] + (c_1c_2 + T_{H1})C_{wf}E_{H1} + C_{wf}(c_4 - c_5)}{C_{wf}T_0} \tag{32}$$

$$\eta = 1 - \frac{C_{wf}[c_1c_2\eta_{\text{com1}} / (\eta_{\text{com1}} + x - 1) + c_3 - c_4 + c_5]}{C_{H2}E_{H2}[c_1c_2 + T_{H3} - (c_1c_2 + T_{H1})] + C_{wf}E_{H1}(c_1c_2 + T_{H1})} \tag{33}$$

where c_1, c_2, c_3, c_4 and c_5 are listed in Appendix A.

When $\eta_{\text{com1}} = \eta_{\text{com2}} = \eta_{\text{tur1}} = \eta_{\text{tur2}} = 1$ and $C_{H1} = C_{H2} = C_{L1} = C_{L2} \to \infty$, Equations (28) and (29) can be reduced to the dimensionless PO and TEF of a modified closed endoreversible binary Brayton cycle with two isothermal heating processes and coupled to CTRs [62]:

$$\bar{W} = \frac{-C_{wf}[d_1d_2 / x + c_3] + C_{H2}E_{H2}\left[d_1d_2 + T_{H3} - E_{H1}(d_1d_2 + T_{H1})\right] + C_{wf}E_{H1}(d_1d_2 + T_{H1}) + C_{wf}(d_4 - d_5)}{C_{wf}T_0} \tag{34}$$

$$\eta = 1 - \frac{C_{wf}(d_1d_2 / x + d_3 - d_4 + d_5)}{C_{H2}E_{H2}[d_1d_2 + T_{H3} - E_{H1}(d_1d_2 + T_{H1})] + C_{wf}E_{H1}(d_1d_2 + T_{H1})} \tag{35}$$

where d_1, d_2, d_3, d_4 and d_5 are listed in Appendix A.

When $E_{R1} = E_{R2} = E_{L2} = 0$, Equations (28) and (29) can be reduced to the dimensionless PO and TEF of a modified closed irreversible Brayton cycle with an isothermal heating process and coupled to VTHRs:

$$\bar{W} = \frac{\begin{array}{l} C_{wf}xy(C_{H2}E_{H2}T_{H3} + C_{L1min}E_{L1}T_{L1}) + C_{H1min}E_{H1}T_{H1}\{[C_{wf} - C_{H2}E_{H2} + C_{L1min}E_{L1}(\eta_{\text{tur1}} - 1)] \\ xy - C_{L1min}E_{L1}\eta_{\text{tur1}}\} + e\{-xy[C_{H1min}C_{wf}E_{H1} + C_{H2}E_{H2}(C_{wf} - C_{H1min}E_{H1})] + C_{L1min}E_{L1}(C_{wf} \\ -C_{H1min}E_{H1})[(\eta_{\text{tur1}} - 1)xy - \eta_{\text{tur1}}]\} \end{array}}{C_{wf}^2T_0xy} \tag{36}$$

$$\eta = \frac{\begin{array}{l} C_{H1min}C_{L1min}E_{H1}E_{L1}\eta_{\text{tur1}}T_{H1} - xy\{C_{H1min}E_{H1}T_{H1}[C_{wf} - C_{H2}E_{H2} + C_{L1min}E_{L1}(\eta_{\text{tur1}} - 1)] + C_{wf} \\ (C_{H2}E_{H2}T_{H3} + C_{L1min}E_{L1}T_{L1})\} + e\{xy[C_{H1min}C_{wf}E_{H1} + C_{H2}E_{H2}(C_{wf} - C_{H1min}E_{H1})] - E_{L1} \\ C_{L1min}(C_{wf} - C_{H1min}E_{H1})[(\eta_{\text{tur1}} - 1)xy - \eta_{t1}]\} \end{array}}{\begin{array}{l} xy\{e_1e_2[C_{H2}C_{wf}E_{H2} + C_{H1min}E_{H1}(C_{wf} - C_{H2}E_{H2})] + C_{H1min}E_{H1}T_{H1}(C_{H2}E_{H2} - C_{wf}) - \\ C_{H2}C_{wf}E_{H2}T_{H3}\} \end{array}} \tag{37}$$

where e is listed in Appendix A.

When $E_{R1} = E_{R2} = E_{L2} = 0$ and $C_{H1} = C_{H2} = C_{L1} \to \infty$, Equations (28) and (29) can be reduced to the dimensionless PO and TEF of a modified closed irreversible Brayton cycle with an isothermal heating process and coupled to CTRs:

$$\bar{W}=\frac{\begin{array}{l}xy(C_{H2}E_{H2}T_{H3}+C_{wf}E_{L1}T_{L1})+E_{H1}T_{H1}\{[C_{wf}-C_{H2}E_{H2}+C_{wf}E_{L1}(\eta_{\text{tur1}}-1)]xy-C_{wf}\\ E_{L1}\eta_{\text{tur1}}\}+b_1b_2\{E_LC_{wf}(1-E_H)[(\eta_{\text{tur1}}-1)xy-\eta_{\text{tur1}}]-[C_{wf}E_H+C_{H2}E_{H2}(1-E_{H1})]xy\}\end{array}}{C_{wf}T_0xy} \tag{38}$$

$$\eta=\frac{\begin{array}{l}C_{wf}E_{H1}E_{L1}\eta_{\text{tur1}}T_{H1}-xy\{E_{H1}T_{H2}[C_{wf}-C_{H2}E_{H2}+C_{wf}E_{L1}(\eta_{\text{tur1}}-1)]+(C_{H2}E_{H2}T_{H3}+C_{wf}E_{L1}\\ T_{L1})\}+b_1b_2\{[C_{wf}E_{H1}+C_{H2}(1-E_{H1})E_{H2}]xy-C_{wf}E_{L2}(1-E_{H1})[xy(\eta_{\text{tur1}}-1)-\eta_{\text{tur1}}]\}\end{array}}{xy\{b_1b_2[C_{H2}E_{H2}+E_{H1}(C_{wf}-C_{H2}E_{H2})]+E_{H1}(C_{H2}E_{H2}-C_{wf})T_{H1}-C_{H2}E_{H2}T_{H3}\}} \tag{39}$$

When $E_{R1}=E_{R2}=E_{L2}=0$ and $\eta_{\text{com1}}=\eta_{\text{tur1}}=1$, Equations (28) and (29) can be reduced to the dimensionless PO and TEF of a modified closed endoreversible Brayton cycle with an isothermal heating process and coupled to VTHRs [59,60]:

$$\bar{W}=\frac{\begin{array}{l}C_{wf}x\{C_{L1min}C_{wf}E_{L1}T_{L1}(y-1)+C_{H2}E_{H2}\cdot[C_{wf}T_{H3}(y-1)+C_{L1min}E_{L1}T_{H3}T_{L1}xy]\}+C_{H1min}\\ E_{H1}\{C_{L1min}E_{L1}[C_{wf}T_{H1}(x-1)+C_{wf}T_{L1}x(1-xy)+C_{H2}E_{H2}x(T_{L1}xy-T_{H3})]+C_{wf}x[C_{wf}\\ T_{H1}(y-1)+C_{H2}E_{H2}(T_{H3}-T_{H1}y)]\}\end{array}}{C_{wf}T_0x[C_{wf}^2y-(C_{wf}-C_{H1min}E_{H1})(C_{wf}-C_{L1min}E_{L1})]} \tag{40}$$

$$\eta=\frac{\begin{array}{l}C_{wf}T_0x\{C_{L1min}C_{wf}E_{L1}T_{L1}(y-1)+C_{H2}E_{H2}[C_{wf}T_{H3}(y-1)+C_{L1min}E_{L1}(T_{H3}-T_{L1}xy)]\}+\\ C_{H1min}E_{H1}\{C_{L1min}E_{L1}[C_{wf}T_{H1}(x-1)+C_{wf}T_{L1}x(1-xy)+C_{H2}E_{H2}x(T_{L1}xy-T_{H3})]+C_{wf}\\ x[C_{wf}T_{H1}(y-1)+C_{H2}E_{H2}(T_{H3}-T_{H1}y)]\}\end{array}}{\begin{array}{l}C_{wf}T_0x\{C_{H1min}E_{H1}[C_{wf}^2T_{H1}(y-1)+C_{H2}C_{wf}E_{H2}(T_{H3}-T_{H1}y)+C_{L1min}C_{wf}E_{L1}(T_{H1}-T_{L1}xy)\\ +C_{H2}C_{L1min}E_{H2}E_{L1}(T_{L1}xy-T_{H3})]+C_{H2}C_{wf}E_{H2}[C_{wf}T_{H3}(y-1)+C_{L1min}E_{L1}(T_{H3}-T_{L1}xy)]\}\end{array}} \tag{41}$$

When $E_{R1}=E_{R2}=E_{L2}=0$, $C_{H1}=C_{H2}=C_{L1}\to\infty$ and $\eta_{\text{com1}}=\eta_{\text{tur1}}=1$, Equations (28) and (29) can be reduced to the dimensionless PO and TEF of a modified closed endoreversible Brayton cycle with an isothermal heating process and coupled to CTRs:

$$\bar{W}=\frac{\begin{array}{l}x\{C_{wf}E_{L1}T_{L1}(y-1)+C_{H2}E_{H2}[T_{H3}(y-1)+E_{L1}T_{H3}T_{L1}xy]\}+E_{H1}\{E_{L1}[C_{wf}T_{H1}(x-1)+\\ C_{wf}T_{L1}x(1-xy)+C_{H2}E_{H2}x(T_{L1}xy-T_{H3})]+x[C_{wf}T_{H1}(y-1)+C_{H2}E_{H2}(T_{H3}-T_{H1}y)]\}\end{array}}{C_{wf}T_0x[y-(1-E_{H1})(1-E_{L1})]} \tag{42}$$

$$\eta=\frac{\begin{array}{l}T_0x\{C_{wf}E_{L1}T_{L1}(y-1)+C_{H2}E_{H2}[T_{H3}(y-1)+E_{L1}(T_{H3}-T_{L1}xy)]\}+E_{H1}\{E_{L1}[C_{wf}T_{H1}(x-1)\\ +C_{wf}T_{L1}x(1-xy)+C_{H2}E_{H2}x(T_{L1}xy-T_{H3})]+x[C_{wf}T_{H1}(y-1)+C_{H2}E_{H2}(T_{H3}-T_{H1}y)]\}\end{array}}{\begin{array}{l}C_{wf}T_0x\{E_{H1}[C_{wf}T_{H1}(y-1)+C_{H2}E_{H2}(T_{H3}-T_{H1}y)+C_{wf}E_{L1}(T_{H1}-T_{L1}xy)+C_{H2}E_{H2}E_{L1}\\ (T_{L1}xy-T_{H3})]+C_{H2}E_{H2}[T_{H3}(y-1)+E_L\left(T_{H3}-T_{L1}xy\right)]\}\end{array}} \tag{43}$$

When $E_{H2}=E_{R1}=E_{R2}=E_{L2}=0$, Equations (28) and (29) can be reduced to the dimensionless PO and TEF of a closed irreversible simple Brayton cycle coupled to VTHRs [37,63]:

$$\bar{W}=\frac{\begin{array}{l}\{\eta_{\text{com1}}C_{wf}-(1-\eta_{\text{tur1}}+\eta_{\text{tur1}}/x)[(C_{wf}-C_{L1\min}E_{L1})(x-1+\eta_{\text{com1}})+\eta_{\text{com1}}C_{L1\min}E_{L1}]\}C_{H1\min}E_{H1}\\ \tau_{H1}-\{(x-1+\eta_{\text{com1}})[(C_{wf}-C_{H1\min}E_{H1})(1-\eta_{\text{tur1}}+\eta_{\text{tur1}}/x)+C_{H1\min}E_{H1}]-\eta_{\text{com1}}C_{wf}\}C_{L1\min}E_{L1}\end{array}}{\eta_{\text{com1}}C_{wf}{}^2-(x-1+\eta_{\text{com1}})(C_{wf}-C_{H1\min}E_{H1})(C_{wf}-C_{L1\min}E_{L1})(1-\eta_{\text{tur1}}+\eta_{\text{tur1}}/x)} \tag{44}$$

$$\eta=1-\frac{E_{L1}[E_{H1}\eta_{\text{com1}}\tau_{H1}(1-\eta_{\text{tur1}}+\eta_{\text{tur1}}/x)-\eta_{\text{com1}}+(x-1+\eta_{\text{com1}})(1-E_{H1})(1-\eta_{\text{tur1}}+\eta_{\text{tur1}}/x)]}{E_{H1}\{\tau_{H1}[\eta_{\text{com1}}-(x-1+\eta_{\text{com1}})(1-E_{L1})(1-\eta_{\text{tur1}}+\eta_{\text{tur1}}/x)]-E_{L1}(x-1+\eta_{\text{com1}})\}} \tag{45}$$

When $E_{H2}=E_{R1}=E_{R2}=E_{L2}=0$ and $C_{H1}=C_{H2}=C_{L1}\to\infty$, Equations (28) and (29) can be reduced to the dimensionless PO and TEF of a closed irreversible simple Brayton cycle coupled to CTRs [37,63]:

$$\bar{W}=\frac{\begin{array}{l}\{E_{H1}\tau_{H1}\{\eta_{\text{com1}}-(1-\eta_{\text{tur1}}+\eta_{\text{tur1}}/x)[(x-1+\eta_{\text{com1}})(1-E_{L1})+\eta_{\text{com1}}E_{L1}]\}-\{(x-1+\eta_{\text{com1}})\\ [(1-\eta_{\text{tur1}}+\eta_{\text{tur1}}/x)(1-E_{H1})+E_{H1}]-\eta_{\text{com1}}\}E_{L1}\}\end{array}}{\eta_{\text{com1}}-(x-1+\eta_{\text{com1}})(1-E_{H1})(1-E_{L1})(1-\eta_{\text{tur1}}+\eta_{\text{tur1}}/x)} \tag{46}$$

$$\eta = 1 - \frac{E_{L1}[\eta_{\mathrm{com1}} E_{H1} \tau_{H1} (1-\eta_{\mathrm{tur1}} + \eta_{\mathrm{tur1}} / x) - \eta_{\mathrm{com1}} + (x-1+\eta_{\mathrm{com1}})(1-E_{H1})(1-\eta_{\mathrm{tur1}} + \eta_{\mathrm{tur1}} / x)]}{E_{H1}\{[\eta_{\mathrm{com1}} - (x-1+\eta_{\mathrm{com1}})(1-E_{L1})(1-\eta_{\mathrm{tur1}} + \eta_{\mathrm{tur1}} / x)]\tau_{H1} - E_{L1}(x-1+\eta_{\mathrm{com1}})\}} \tag{47}$$

When $E_{H2} = E_{R1} = E_{R2} = E_{L2} = 0$ and $\eta_{\mathrm{com1}} = \eta_{\mathrm{tur1}} = 1$, Equations (28) and (29) can be reduced to the dimensionless PO and TEF of a closed endoreversible simple Brayton cycle coupled to VTHRs [64]:

$$\bar{W} = \frac{C_{H1min} C_{L1min} E_{H1} E_{L1} (x-1)(\tau_{H1} - x\tau_{L1})}{C_{L1min} C_{wf} E_{L1} + C_{H1min} E_{H1} (C_{wf} - C_{L1min} E_{L1})} \tag{48}$$

$$\eta = 1 - x^{-1} \tag{49}$$

When $E_{H2} = E_{R1} = E_{R2} = E_{L2} = 0$, $\eta_{\mathrm{com1}} = \eta_{\mathrm{tur1}} = 1$ and $C_{H1} = C_{H2} = C_{L1} \to \infty$, Equations (28) and (29) can be reduced to the dimensionless PO and TEF of the closed endoreversible simple Brayton cycle coupled to CTRs [65,66]:

$$\bar{W} = \frac{E_{H1} E_{L1} (1 - 1/x)(\tau_{H1} - x\tau_{L1})}{E_{H1} + E_{L1} - E_{H1} E_{L1}} \tag{50}$$

$$\eta = 1 - x^{-1} \tag{51}$$

3. Optimal Heat Conductance Distributions

With $\bar{W}$ as the optimization objective, the heat conductances of six heat exchangers will be optimized by fixing the total heat conductance (THC); namely, $U_T = \sum U_j$ ($j = H1, H2, R1, R2, L1, L2$). The HCDs in the RCC, CCC, OR, IR, PC1 and PC2 are defined as:

$$u_j = U_j / U_T \tag{52}$$

where u_j must meet the following constraints:

$$\sum u_j = 1, 0 < u_j < 1 \tag{53}$$

The dimensionless PO of the MCBBC can be maximized by optimizing the HCDs. Finally, the maximum dimensionless PO ($\bar{W}_{\max}$) and the corresponding optimal HCDs ($(u_{H1})_{\bar{W}_{\max}}$, $(u_{H2})_{\bar{W}_{\max}}$, $(u_{L1})_{\bar{W}_{\max}}$, $(u_{L2})_{\bar{W}_{\max}}$, $(u_{R1})_{\bar{W}_{\max}}$ and $(u_{R2})_{\bar{W}_{\max}}$) can be obtained. Moreover, the optimal isothermal pressure drop ratios ($(\pi_t)_{\bar{W}_{\max}}$ and $(\pi_{ta})_{\bar{W}_{\max}}$) can be calculated based on the optimal HCDs. The values or ranges of the variables are listed in Table 1. The flow chart of dimensionless PO optimization is displayed in Figure 2. Calculate the negative number of the dimensionless power output, and then the function "fmincon" in MATLAB is used to solve the minimum value. The parameters of "fmincon" are: "TolCon" is 10^{-6}, "TolConSQP" is 300 and "TolFun" is 10^{-6}.

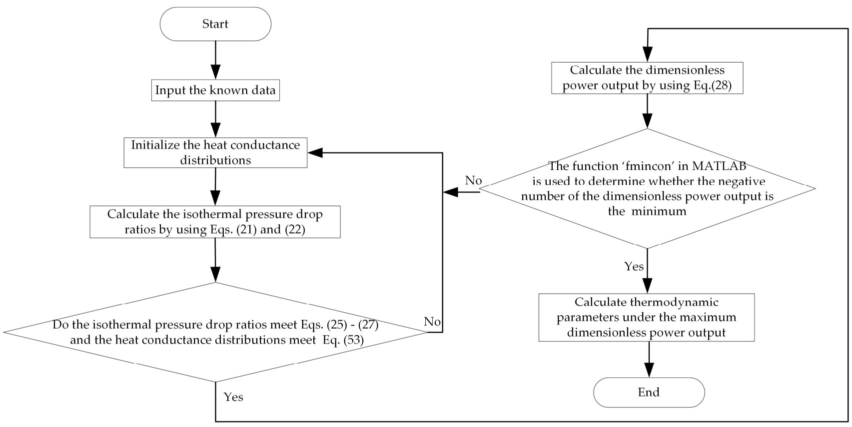

Figure 2. Flow chart of dimensionless power output (PO) optimization.

Figures 3a,b, 4a,b, 5a,b and 6 illustrate the relationships of the maximum dimensionless PO ($\bar{W}_{\max}$), the corresponding dimensionless PO $(\bar{W}_{\mathrm{top}})_{\bar{W}_{\max}}$ of the topping cycle, dimensionless PO $(\bar{W}_{\mathrm{bot}})_{\bar{W}_{\max}}$ of the bottoming cycle, TEF $\eta_{\bar{W}_{\max}}$, isothermal pressure drop ratios ($(\pi_t)_{\bar{W}_{\max}}$ and $(\pi_{ta})_{\bar{W}_{\max}}$) and HCDs ($(u_{H1})_{\bar{W}_{\max}}$, $(u_{H2})_{\bar{W}_{\max}}$, $(u_{L1})_{\bar{W}_{\max}}$, $(u_{L2})_{\bar{W}_{\max}}$, $(u_{R1})_{\bar{W}_{\max}}$ and $(u_{R2})_{\bar{W}_{\max}}$) versus the pressure ratios (π_{com1} and π_{com2}) in the Com1 and Com2, respectively.

Table 1. Values or ranges of the variables.

Parameters	Symbol	Initial Value	Range	Unit
Thermal capacity rate of outer fluid at RCC	C_{H1}	1.2	——	kW / K
Thermal capacity rate of outer fluid at CCC	C_{H2}	1	——	kW / K
Thermal capacity rate of outer fluid at PC1	C_{L1}	1.2	——	kW / K
Thermal capacity rate of outer fluid at PC2	C_{L2}	1.2	——	kW / K
Thermal capacity rate of WF	C_{wf}	1	——	kW / K
Specific heats ratio	k	1.4	——	——
Gas constant	R_g	0.287	——	kJ / (kg · K)
Ambient temperature	T_0	300	——	K
THC	U_{tot}	18	8–36	kW / K
Compressor efficiencies	η_{com1}, η_{com2}	0.9	0.7–1	——
Turbine efficiencies	η_{tur1}, η_{tur2}	0.9	0.7–1	——
Inlet temperature ratio of outer fluid at RCC	τ_{H1}	4	3–6.67	——
Inlet temperature ratio of outer fluid at CCC	τ_{H3}	5	3–6.67	——
Inlet temperature ratio of outer fluid at PC1	τ_{L1}	1	——	——
Inlet temperature ratio of outer fluid at PC2	τ_{L3}	1	——	——
Pressure ratio at Com1	π_{c1}	——	2–20	——
Pressure ratio at Com2	π_{c2}	——	1–6	——

Figure 3a shows that $\bar{W}_{\max}$ increases first and then decreases as π_{com1} or π_{com2} increases. There is a set of optimal pressure ratios ($(\pi_{\mathrm{com1}})_{\bar{W}_{\max,2}}$ and $(\pi_{\mathrm{com2}})_{\bar{W}_{\max,2}}$), so that $\bar{W}_{\max}$ achieves the double maximum dimensionless PO $\bar{W}_{\max,2}$. This is because when π_{com1} gradually increases, $\dot{Q}_{2-3}$, $\dot{Q}_{7-1}$ and $\dot{Q}_{5a-1a}$ gradually reduce, and $\dot{Q}_{3-4}$ slightly increases. With the increase in π_{com2}, $\dot{Q}_{2-3}$ decreases, $\dot{Q}_{3-4}$ decreases slightly, $\dot{Q}_{7-1}$ decreases first and then increases, and $\dot{Q}_{5a-1a}$ decreases. Under the given conditions, $\bar{W}_{\max,2}$, $(\pi_{\mathrm{com1}})_{\bar{W}_{\max,2}}$ and $(\pi_{\mathrm{com2}})_{\bar{W}_{\max,2}}$ are approximately 1.01, 7.7 and 2.8, respectively.

Figure 3b shows that $(\bar{W}_{\mathrm{top}})_{\bar{W}_{\max}}$ increases first; then decreases as π_{com1} increases; and remains substantially unchanged with the change of π_{com2}. $(\bar{W}_{\mathrm{bot}})_{\bar{W}_{\max}}$ decreases at first and then tends to remain unchanged with the increase in π_{com1}, the value of which is much smaller than that of $(\bar{W}_{\mathrm{top}})_{\bar{W}_{\max}}$. This is because T_5 decreases at first and then tends to be constant as π_{com1} increases. As π_{com2} increases, $(\bar{W}_{\mathrm{bot}})_{\bar{W}_{\max}}$ increases at first and then tends to be constant when π_{com1} is smaller; $(\bar{W}_{\mathrm{bot}})_{\bar{W}_{\max}}$ increases at first and then decreases to zero when π_{com1} is larger. That is, $\dot{Q}_{2a-3a}$ and $\dot{Q}_{3a-4a}$ can only be used to maintain the operation of the bottoming cycle. Figure 4a shows that $\eta_{\bar{W}_{\max}}$ increases at first and then becomes constant with the increase in π_{com1} or π_{com2}.

Figure 4b shows that $(\pi_t)_{\bar{W}_{\max}}$ remains unchanged as π_{com1} or π_{com2} increases, and is always located at the lower limit. This indicates that the degree of the isothermal heating in CCC always reaches the maximum. Therefore, $\dot{Q}_{3-4}$ only slightly changes with the change of π_{com1} or π_{com2}.

When π_{com1} or π_{com2} is smaller, $(\pi_{ta})_{\bar{W}_{\max}}$ decreases slightly with the increase in π_{com1} and reaches the lower limit with the increase in π_{com2}. That indicates that under this condition, the degree of the isothermal heating in IR increases as π_{com1} or π_{com2} does; when π_{com1} and π_{com2} are larger, $(\pi_{ta})_{\bar{W}_{\max}}$ increases with the increase in π_{com1} or π_{com2}; when $(\bar{W}_{\mathrm{bot}})_{\bar{W}_{\max}}$ is zero, $(\pi_{ta})_{\bar{W}_{\max}}$ remains substantially unchanged as π_{com1} or π_{com2} increases.

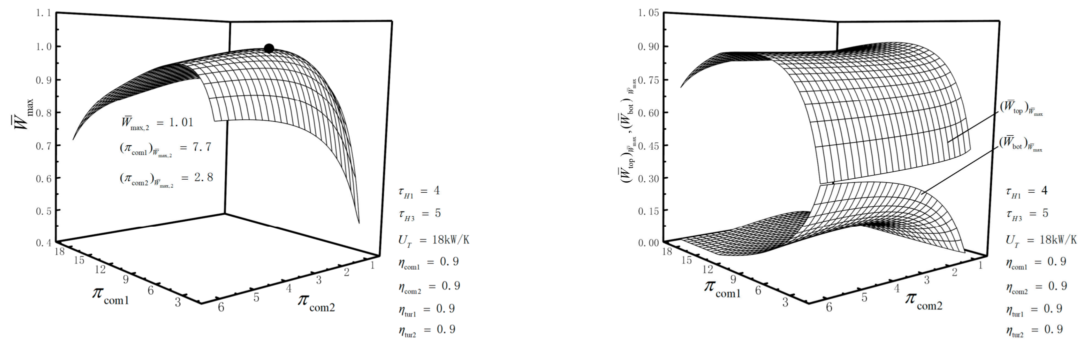

(**a**) (**b**)

Figure 3. (**a**) Relationships of $\bar{W}_{\max}$ versus π_{com1} and π_{com2}; (**b**) relationships of $(\bar{W}_{\mathrm{top}})_{\bar{W}_{\max}}$ and $(\bar{W}_{\mathrm{bot}})_{\bar{W}_{\max}}$ versus π_{com1} and π_{com2}.

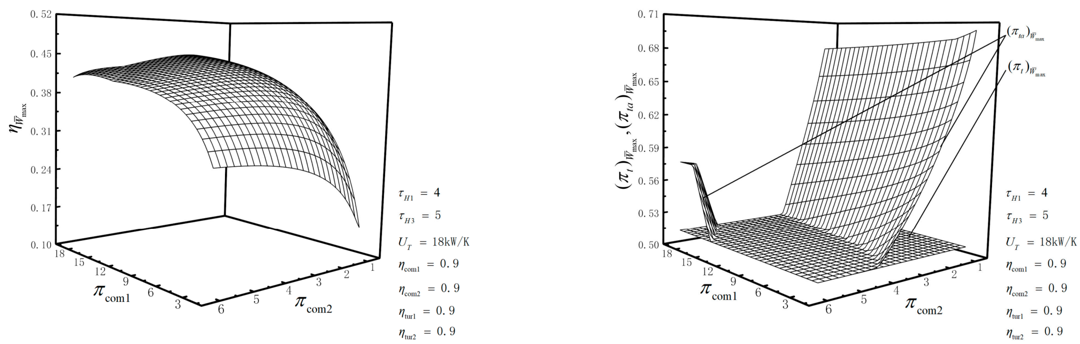

(**a**) (**b**)

Figure 4. (**a**) Relationships of $\eta_{\bar{W}_{\max}}$ versus π_{com1} and π_{com2}; (**b**) relationships of $(\pi_t)_{\bar{W}_{\max}}$ and $(\pi_{ta})_{\bar{W}_{\max}}$ versus π_{com1} and π_{com2}.

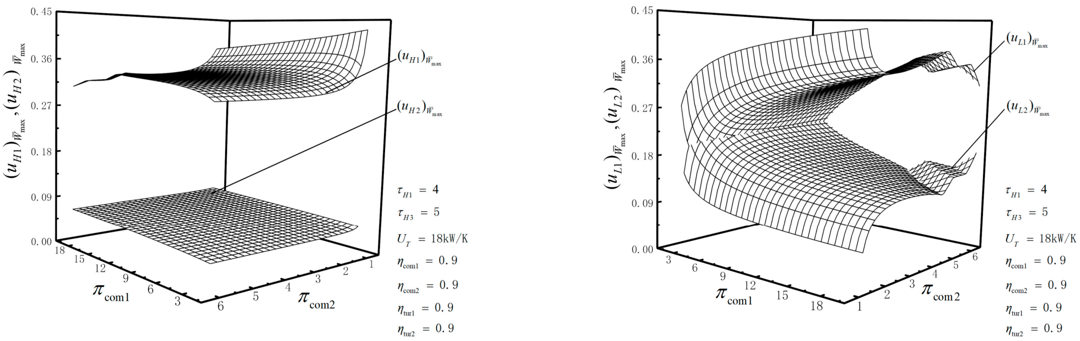

(**a**) (**b**)

Figure 5. (**a**) Relationships of $(u_{H1})_{\bar{W}_{\max}}$ and $(u_{H2})_{\bar{W}_{\max}}$ versus π_{com1} and π_{com2}; (**b**) relationships of $(u_{L1})_{\bar{W}_{\max}}$ and $(u_{L2})_{\bar{W}_{\max}}$ versus π_{com1} and π_{com2}.

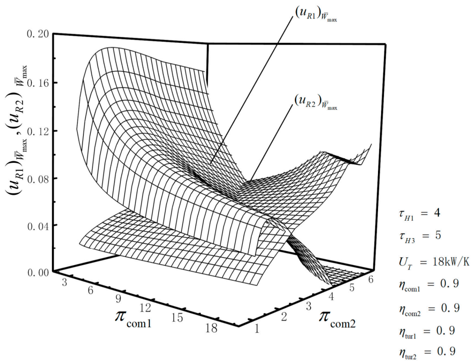

Figure 6. Relationships of $(u_{R1})_{\bar{W}_{\max}}$ and $(u_{R2})_{\bar{W}_{\max}}$ versus π_{com1} and π_{com2}.

Figure 5a shows that when $(u_{R1})_{\bar{W}_{\max}}$ is not zero, $(u_{H1})_{\bar{W}_{\max}}$ increases slightly at first and then decreases slightly with the increase in π_{com1}; $(u_{H1})_{\bar{W}_{\max}}$ decreases first and then tends to remain unchanged with the increase in π_{com2}. When $(u_{R1})_{\bar{W}_{\max}}$ is zero but both of $(\pi_{ta})_{\bar{W}_{\max}}$ and $(\bar{W}_{\text{bot}})_{\bar{W}_{\max}}$ are not zero, $(u_{H1})_{\bar{W}_{\max}}$ decreases as π_{com1} or π_{com2} increases; when both of $(u_{R1})_{\bar{W}_{\max}}$ and $(\pi_{ta})_{\bar{W}_{\max}}$ are zero but $(\bar{W}_{\text{bot}})_{\bar{W}_{\max}}$ is not zero, changing π_{com1} or π_{com2} does not change $(u_{H1})_{\bar{W}_{\max}}$; when $(u_{R1})_{\bar{W}_{\max}}$, $(\pi_{ta})_{\bar{W}_{\max}}$ and $(\bar{W}_{\text{bot}})_{\bar{W}_{\max}}$ are zero, $(u_{H1})_{\bar{W}_{\max}}$ decreases with the increase in π_{com1} or π_{com2}. $(u_{H2})_{\bar{W}_{\max}}$ has nothing to do with π_{com1} or π_{com2}, and is far less than $(u_{H1})_{\bar{W}_{\max}}$. With the decrease in $(u_{H1})_{\bar{W}_{\max}}$, E_{H1} decreases, and then $\dot{Q}_{2-3}$ decreases. $(u_{H2})_{\bar{W}_{\max}}$ remains basically unchanged, E_{H2} is constant and the variation of $\dot{Q}_{3-4}$ is very small.

Figure 5b shows that when $(u_{R1})_{\bar{W}_{\max}}$ is not zero, $(u_{L1})_{\bar{W}_{\max}}$ increases as π_{com1} increases; it decreases first and then increases slightly as π_{com2} increases; $(u_{L2})_{\bar{W}_{\max}}$ decreases first and tends to remain unchanged with the increase in π_{com1}; it increases first and then tends to be the same with the increase in π_{com2}. When $(u_{R1})_{\bar{W}_{\max}}$ is zero but both of $(\pi_{ta})_{\bar{W}_{\max}}$ and $(\bar{W}_{\text{bot}})_{\bar{W}_{\max}}$ are not zero, $(u_{L1})_{\bar{W}_{\max}}$ decreases sharply with the increase in π_{com1} or π_{com2}, while $(u_{L2})_{\bar{W}_{\max}}$ increases sharply with the increase in π_{com1} or π_{com2}. When both of $(u_{R1})_{\bar{W}_{\max}}$ and $(\pi_{ta})_{\bar{W}_{\max}}$ are zero but $(\bar{W}_{\text{bot}})_{\bar{W}_{\max}}$ is not zero, $(u_{L1})_{\bar{W}_{\max}}$ increases slightly with the increase in π_{com1} or π_{com2}, and $(u_{L2})_{\bar{W}_{\max}}$ remains basically unchanged with the increase in π_{com1} or π_{com2}. When $(u_{R1})_{\bar{W}_{\max}}$, $(\pi_{ta})_{\bar{W}_{\max}}$ and $(\bar{W}_{\text{bot}})_{\bar{W}_{\max}}$ are zero, $(u_{L1})_{\bar{W}_{\max}}$ decreases and $(u_{L2})_{\bar{W}_{\max}}$ increases as π_{com1} or π_{com2} increases.

Figure 6 shows that $(u_{R1})_{\bar{W}_{\max}}$ decreases to zero with the increase in π_{com1}, and increases at first and then decreases to zero as π_{com2} increases. When $(\pi_{ta})_{\bar{W}_{\max}}$ is not zero, $(u_{R2})_{\bar{W}_{\max}}$ increases with the increase in π_{com1} or π_{com2}. When $(\pi_{ta})_{\bar{W}_{\max}}$ is zero but $(\bar{W}_{\text{bot}})_{\bar{W}_{\max}}$ is not zero, $(u_{R2})_{\bar{W}_{\max}}$ decreases with the increase in π_{com1} or π_{com2}. When both of $(\pi_{ta})_{\bar{W}_{\max}}$ and $(\bar{W}_{\text{bot}})_{\bar{W}_{\max}}$ are zero, $(u_{R2})_{\bar{W}_{\max}}$ increases with the increase in π_{com1} or π_{com2}. Because increasing $(u_{R2})_{\bar{W}_{\max}}$ leads to the increases in E_{R2} and $\dot{Q}_{3a-4a}$ so as to avoid the negative value of $(\bar{W}_{\text{bot}})_{\bar{W}_{\max}}$, namely, inverse dimensionless PO of the bottoming cycle.

According to the numerical calculation, the influences of the temperature ratios, compressor efficiencies, turbine efficiencies and THC on optimization results are further analyzed. Figure 7a,b illustrates the relationships of the double maximum dimensionless PO ($\bar{W}_{\max,2}$) and the corresponding TEF ($\eta_{\bar{W}_{\max,2}}$) versus the temperature ratios (τ_{H1} and τ_{H3}). As can be seen from figure 7a,b, both $\bar{W}_{\max,2}$ and $\eta_{\bar{W}_{\max,2}}$ increase first and then tend to be unchanged with the increase in π_{com1} or π_{com2}. There is an optimal temperature ratio $(\tau_{H3})_{\text{opt}}$ which makes $\bar{W}_{\max,2}$ reach the optimal. The corresponding fitting expression is $(\tau_{H3})_{\text{opt}} = 1.1\tau_{H1} + 0.14$, and the correlation coefficient is $r = 0.9964$. As for $\eta_{\bar{W}_{\max,2}}$, there also exists $(\tau_{H3})_{\text{opt}}$ that satisfies the fitting expression: $(\tau_{H3})_{\text{opt}} = 1.1\tau_{H1} + 0.18$, and its correlation coefficient is also $r = 0.9964$. In the actual design process, τ_{H1} and τ_{H3} should meet the relationship similar to $(\tau_{H3})_{\text{opt}} = 1.1\tau_{H1} + 0.14$ or $(\tau_{H3})_{\text{opt}} = 1.1\tau_{H1} + 0.18$, in order to obtain as much $\bar{W}_{\max,2}$ and $\eta_{\bar{W}_{\max,2}}$ as possible and reduce the requirement for high temperature resistances of materials.

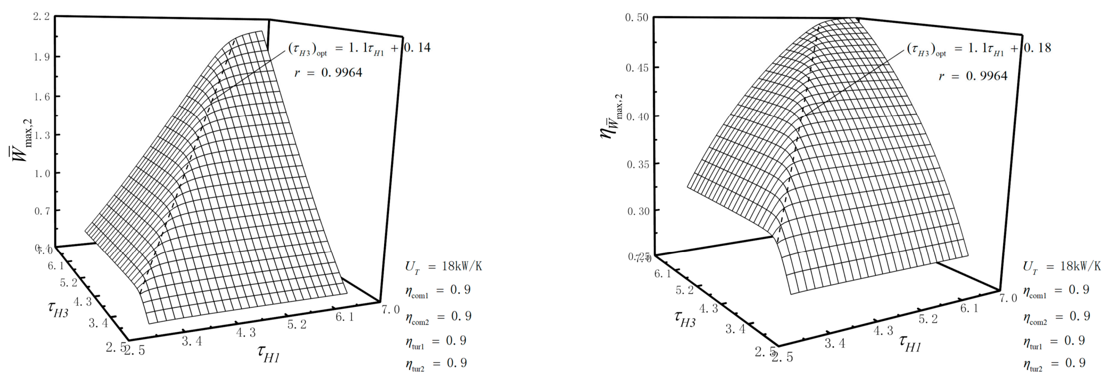

(**a**) (**b**)

Figure 7. (**a**) Relationships of $\bar{W}_{\max,2}$ versus τ_{H1} and τ_{H3}; (**b**) relationships of $\eta_{\bar{W}_{\max}}$ versus τ_{H1} and τ_{H3}.

Figure 8a illustrates the relationships of $\bar{W}_{\max,2}$, $(\bar{W}_{\text{top}})_{\bar{W}_{\max,2}}$, $(\bar{W}_{\text{bot}})_{\bar{W}_{\max,2}}$ and $\eta_{\bar{W}_{\max,2}}$ versus η_{com2}. It shows that $\bar{W}_{\max,2}$, $\eta_{\bar{W}_{\max,2}}$ and $(\bar{W}_{\text{bot}})_{\bar{W}_{\max,2}}$ increase and $(\bar{W}_{\text{top}})_{\bar{W}_{\max,2}}$ decreases slightly with the increase in η_{com2}. With the increase in η_{com2}, $\dot{Q}_{2-3}$ and $\dot{Q}_{7-1}$ basically increase. With the increase in η_{com2}, $\dot{Q}_{3-4}$ remains substantially unchanged, $\dot{Q}_{5a-1a}$ decreases and $\dot{Q}_{3a-4a}$ increases. The amount of change in $\bar{W}_{\max,2}$ is mainly affected by that in $\dot{Q}_{5a-1a}$. It should be noted that when $\eta_{\text{com2}} \le 0.75$, $\bar{W}_{\max,2}$, $\eta_{\bar{W}_{\max,2}}$, $(\bar{W}_{\text{top}})_{\bar{W}_{\max,2}}$ and $(\bar{W}_{\text{bot}})_{\bar{W}_{\max,2}}$ do not exist and are indicated by dashed lines.

Figure 8b illustrates the relationships of $(\pi_{\text{com1}})_{\bar{W}_{\max,2}}$, $(\pi_{\text{com2}})_{\bar{W}_{\max,2}}$, $(\pi_t)_{\bar{W}_{\max,2}}$ and $(\pi_{ta})_{\bar{W}_{\max,2}}$ versus η_{com2}. It shows that $(\pi_{\text{com1}})_{\bar{W}_{\max,2}}$ decreases and $(\pi_{c2})_{\bar{W}_{\max,2}}$ increases as η_{com2} increases. The decrease in $(\pi_{\text{com1}})_{\bar{W}_{\max,2}}$ reduces T_2, thereby increasing $\dot{Q}_{2-3}$. Under the given condition, T_{4a} is less than T_{5a} when η_{com2} is less than or equal to 0.76. As η_{com2} increases, $(\pi_t)_{\bar{W}_{\max,2}}$ remains the lower limit, which indicates that the degree of the isothermal heating in CCC always reaches the maximum. As η_{com2} increases, $(\pi_{ta})_{\bar{W}_{\max,2}}$ decreases to the lower limit, which indicates that increasing η_{com2} improves the degree of the isothermal heating in IR.

Figure 8c illustrates the relationship of $(u_j)_{\bar{W}_{\max,2}}$ versus η_{com2}. It shows that as η_{com2} decreases, $(u_{H1})_{\bar{W}_{\max,2}}$, $(u_{H2})_{\bar{W}_{\max,2}}$ and $(u_{R1})_{\bar{W}_{\max,2}}$ remains basically unchanged; $(u_{L1})_{\bar{W}_{\max,2}}$ decreases first and then tends to remain unchanged; $(u_{L2})_{\bar{W}_{\max,2}}$ increases first and then tends to be unchanged; $(u_{R2})_{\bar{W}_{\max,2}}$ increases.

Similarly, both of $\bar{W}_{\max,2}$ and $\eta_{\bar{W}_{\max,2}}$ increase as η_{com1}, η_{tur1} and η_{tur2} increase. The effects of η_{com1} and η_{tur1} on $\bar{W}_{\max,2}$ and $\eta_{\bar{W}_{\max,2}}$ are greater than those of η_{com2} and η_{tur2}. $(\bar{W}_{\text{top}})_{\bar{W}_{\max,2}}$ increases with the increases in η_{com1} and η_{tur1}, while $(\bar{W}_{\text{top}})_{\bar{W}_{\max,2}}$ decreases with the increases in η_{com2} and η_{tur2}. $(\bar{W}_{\text{bot}})_{\bar{W}_{\max,2}}$ decreases with the increases in η_{com1} and η_{tur1}, while $(\bar{W}_{\text{top}})_{\bar{W}_{\max,2}}$ increases with the increases in η_{com2} and η_{tur2}. It should be noted that when $\eta_{\text{tur2}} \le 0.74$, $\bar{W}_{\max,2}$, $\eta_{\bar{W}_{\max,2}}$, $(\bar{W}_{\text{top}})_{\bar{W}_{\max,2}}$ and $(\bar{W}_{\text{bot}})_{\bar{W}_{\max,2}}$ also do not exist. When $\eta_{\text{tur2}} > 0.74$, the change of η_{tur2} has little effects on $\bar{W}_{\max,2}$ and $\eta_{\bar{W}_{\max,2}}$. Within the given range, the changes in $\bar{W}_{\max,2}$ and $\eta_{\bar{W}_{\max,2}}$ do not exceed 7% and 4%, respectively. In practical design of improving cycle performance, it is suggested to give priority to appropriately increasing η_{com2} and η_{tur2}. Then one can choose to increase η_{com1} and η_{tur1}, successively. Apart from this, $\bar{W}_{\max,2}$ and $\eta_{\bar{W}_{\max,2}}$ increase as U_T increases.

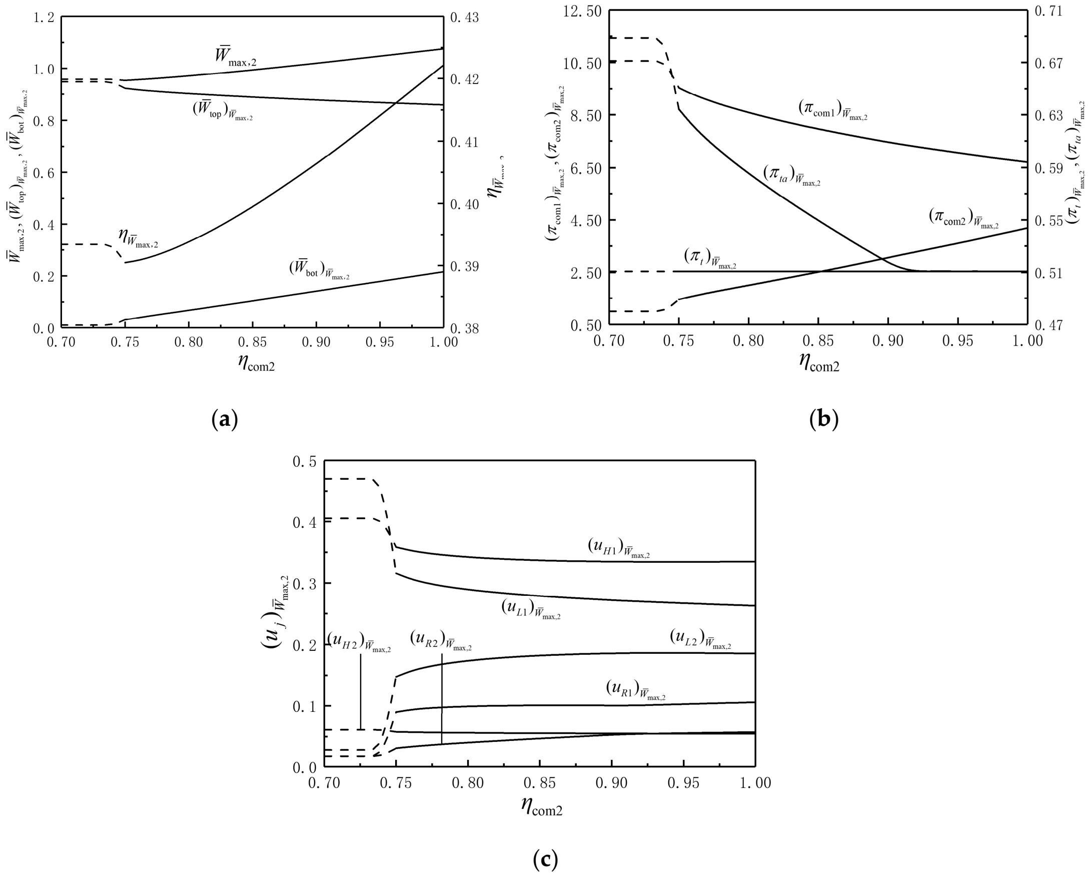

Figure 8. (**a**) Relationships of $\bar{W}_{\max,2}$, $\eta_{\bar{W}_{\max,2}}$, $(\bar{W}_{\text{top}})_{\bar{W}_{\max,2}}$ and $(\bar{W}_{\text{bot}})_{\bar{W}_{\max,2}}$ versus η_{com2}; (**b**) relationships of $(\pi_{\text{com1}})_{\bar{W}_{\max,2}}$, $(\pi_{\text{com2}})_{\bar{W}_{\max,2}}$, $(\pi_t)_{\bar{W}_{\max,2}}$ and $(\pi_{ta})_{\bar{W}_{\max,2}}$ versus η_{com2}; (**c**) relationships of $(u_j)_{\bar{W}_{\max,2}}$ versus η_{com2}.

4. Optimal Thermal Capacitance Rate Matchings

The $\bar{W}$ of the cycle also affected by the TCRMs. By taking $\bar{W}$ as the optimization objective, TCRMs are optimized. Figure 9a,b illustrates the relationships of $\bar{W}_{\max}$ and $\eta_{\bar{W}_{\max}}$. versus C_{H1}/C_{wf} and C_{H2}/C_{wf} when $C_{L1}/C_{H1}=1$ and $C_{L2}/C_{H2}=1.2$. The figures show that both of $\bar{W}_{\max}$ and $\eta_{\bar{W}_{\max}}$ increase, and then tend to remain constant with the increase in C_{H1}/C_{wf} or C_{H2}/C_{wf}. These indicate that there is a set of the optimal C_{H1}/C_{wf} and C_{H2}/C_{wf}, so that $\bar{W}_{\max}$ gets the optimal value. Similarly, there is a set of the optimal C_{H1}/C_{wf} and C_{H2}/C_{wf}, so that $\eta_{\bar{W}_{\max}}$ gets the optimal value.

Figure 10 illustrates that the effects of C_{L1}/C_{H1} on the characteristics of $\bar{W}_{\max}-C_{H1}/C_{wf}$ and $\eta_{\bar{W}_{\max}}-C_{H1}/C_{wf}$ when $C_{H2}=1$ and $C_{L2}/C_{H2}=1.2$. It shows that when $\bar{W}_{\max}$ and $\eta_{\bar{W}_{\max}}$ reach the optimal values, C_{L1}/C_{H1} mainly reduces the corresponding C_{H1}/C_{wf}, and has little effect on the optimal values of $\bar{W}_{\max}$ and $\eta_{\bar{W}_{\max}}$. Similarly, C_{L1}/C_{H1} mainly reduces the corresponding C_{H1}/C_{wf} when $\bar{W}_{\max}$ and $\eta_{\bar{W}_{\max}}$ reach the optimal values, and has little effects on the optimal values of $\bar{W}_{\max}$ and $\eta_{\bar{W}_{\max}}$.

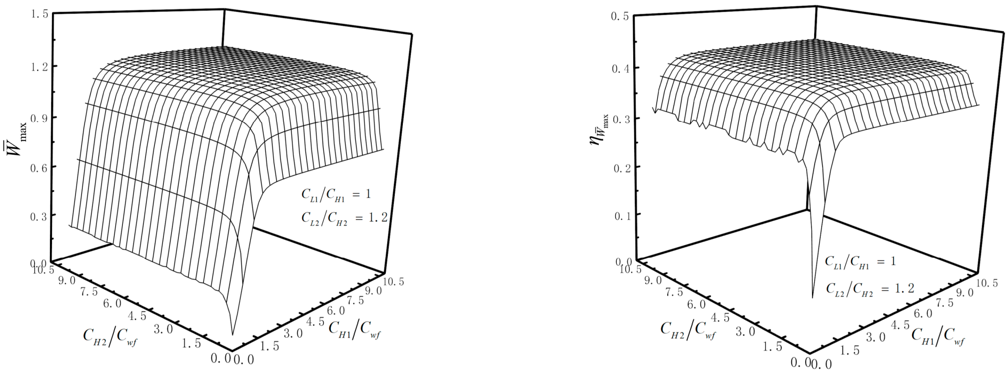

(**a**) (**b**)

Figure 9. (**a**) Relationships of $\bar{W}_{\max}$ versus C_{H1}/C_{wf} and C_{H2}/C_{wf}; (**b**) relationships of $\eta_{\bar{W}_{\max}}$ versus C_{H1}/C_{wf} and C_{H2}/C_{wf}.

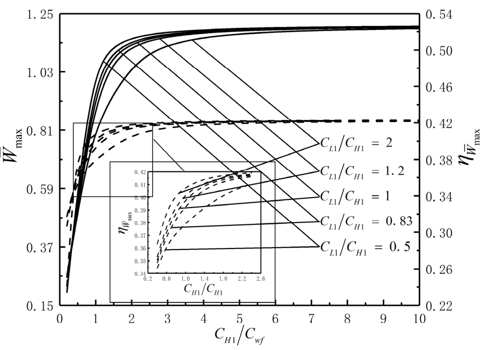

Figure 10. Effects of C_{L1}/C_{H1} on the characteristics of $\bar{W}_{\max} - C_{H1}/C_{wf}$ and $\eta_{\bar{W}_{\max}} - C_{H1}/C_{wf}$.

5. Conclusions

Based on the previous established models in [8,62], a modified closed binary Brayton cycle model coupled to VTHRs with two isothermal heating processes and variable isothermal pressure drop ratios is established by using FTT in this paper. The HCDs of the six heat exchangers are optimized, and the effects of τ_{H1}, τ_{H3}, U_T, η_{com1}, η_{com2}, η_{tur1}, η_{tur2}, C_{H1}/C_{wf} and C_{H2}/C_{wf} on the optimal performances are analyzed by taking $\bar{W}$ as the optimization objective. The results show that there is a set of π_{com1} and π_{com2} which makes $\bar{W}_{\max}$ reach $\bar{W}_{\max,2} = 1.01$. τ_{H1} and τ_{H3} have certain linear relationship ($(\tau_{H3})_{\text{opt}} = 1.1\tau_{H1} + 0.14$, and the correlation coefficient is $r = 0.9964$), which makes $\bar{W}_{\max,2}$ optimal. $\bar{W}_{\max,2}$ increases with the increases in U_T, η_{com1}, η_{com2}, η_{tur1} and η_{tur2}. It should be noted that when $\eta_{\text{com2}} \le 0.75$ or $\eta_{\text{tur2}} \le 0.74$, $\bar{W}_{\max,2}$ does not exist. $\bar{W}_{\max,2}$ increases first and then remain unchanged with the increases in C_{H1}/C_{wf} and C_{H2}/C_{wf}. This cycle can effectively improve energy efficiency and reduce emissions of nitrogen oxide and other harmful gases. Additionally, the optimal results can guide the practical designs for the gas turbine plants.

Author Contributions: C.T., L.C., H.F., W.W. and Y.G. collectively finished the manuscript. All authors have read and agreed to the published version of the manuscript.

Funding: This research was funded the National Natural Science Foundation of China (project number 51779262).

Acknowledgments: The authors wish to thank the reviewers for their careful, unbiased and constructive suggestions, which led to this revised manuscript.

Conflicts of Interest: The authors declare no conflict of interest.

Nomenclature

a, b, c, d, e, m, x, y	Intermediate variables
C	Thermal capacity rate (kW/K)
C_p	Specific heat at constant pressure (kJ/(kg·K))
E	Effectiveness of heat exchanger
k	Specific heat ratio
M	Mach number
N	Number of heat transfer units
$\dot{Q}$	Heat absorbing rate or heat releasing rate
R_g	Gas constant (kJ/(kg·K))
T	Temperature (K)
U	Heat conductance (kW/K)
u	Heat conductance distribution
W	Power output(kW)
$\overline{W}$	Dimensionless power output
Greek symbol	
η	Efficiency
π	Pressure ratio
τ	Temperature ratio
Subscripts	
bot	Bottoming cycle
com	Compressor
H	Hot-side heat exchanger
L	Cold-side heat exchanger
R	Regenerator
s	Isentropic
t/ta	Converging combustion chamber/isothermal regenerator
tot	Total
tur	Turbine
top	Topping cycle
wf	Working fluid
1,2,3,4,5,6,7,1a,2a,3a,4a,5a,2s,5s,2as,5as	State points
Abbreviations	
CCC	Converging combustion chamber
CTR	Constant-temperature reservoir
FTT	Finite-time thermodynamics
HCD	Heat conductance distribution
IR	Isothermal regenerator
MCBBC	Modified closed binary Brayton cycle
PO	Power output
PD	Power density
OR	Ordinary regenerator
RCC	Regular combustion chamber
TCRM	Thermal capacitance rate matching
TEF	Thermal efficiency
THC	Total heat conductance
Tur	Turbine
VTHR	Variable-temperature heat reservoir

WF	Working fluid

Appendix A

$$a_1=\{C_{L2min}E_{L2}[(\eta_{\mathrm{tur2}}-1)x_a y_a-\eta_{\mathrm{tur2}}]\{-C_{wf}(2E_{R1}-1)(E_{R2}-1)(\eta_{\mathrm{com1}}+x-1)[(\eta_{\mathrm{tur1}}-1)xy-\eta_{\mathrm{tur1}}](C_{H1min}E_{H1}+C_{L1min}E_{L1})+C_{H1min}C_{L1min}E_{H1}E_{L1}(2E_{R1}-1)(E_{R2}-1)(\eta_{\mathrm{com1}}+x-1)[(\eta_{\mathrm{tur1}}-1)xy-\eta_{\mathrm{tur1}}]+C_{wf}^2\{(2E_{R1}-1)(E_{R2}-1)(\eta_{\mathrm{com1}}+x-1)\eta_{\mathrm{tur1}}(xy-1)+xy\{E_{R1}[\eta_{\mathrm{com1}}+2x-2-2E_{R2}(\eta_{\mathrm{com1}}+x-1)]+E_{R2}(\eta_{\mathrm{com1}}+x-1)-x+1\}\}\}/\{(\eta_{\mathrm{com1}}+x-1)C_{wf}xy[E_{R1}(2E_{R2}-1)-E_{R2}](C_{wf}-C_{L1min}E_{L1})\}+\{-C_{H1min}E_{H1}(E_{R2}-1)[(\eta_{\mathrm{tur1}}-1)xy-\eta_{\mathrm{tur1}}]\{x_a y_a[-E_{R1}(\eta_{\mathrm{com2}}+2x_a-2)+x_a-1]+(2E_{R1}-1)\eta_{\mathrm{tur2}}(\eta_{\mathrm{com2}}+x_a-1)(x_a y_a-1)\}/(xy)+C_{wf}^2\eta_{\mathrm{com1}}\{x_a y_a[(\eta_{\mathrm{com2}}+x_a-1-E_{R2}\eta_{\mathrm{com2}})E_{R1}-x_a+1]-\eta_{\mathrm{tur2}}(E_{R1}-1)(\eta_{\mathrm{com2}}+x_a-1)(x_a y_a-1)\}/[(\eta_{\mathrm{com1}}+x-1)(C_{wf}-C_{L1min}E_{L1})]+C_{wf}(E_{R2}-1)[(\eta_{\mathrm{tur1}}-1)xy-\eta_{\mathrm{tur1}}]\{(2E_{R1}-1)\eta_{\mathrm{tur2}}(\eta_{\mathrm{com2}}+x_a-1)(x_a y_a-1)+x_a y_a[x_a-1-E_{R1}(\eta_{\mathrm{com2}}+2x_a-2)]\}/(xy)\}/[(-2E_{R1}E_{R2}+E_{R1}+E_{R2})(\eta_{\mathrm{com2}}+x_a-1)]\}/(x_a y_a)$$

$$a_2=\{\{x_a y_a\{C_{L1min}E_{L1}\{C_{L2min}E_{L2}(\eta_{\mathrm{com2}}+x_a-1)[E_{R1}T_{L3}(2E_{R2}-1)+(E_{R1}-1)(\eta_{\mathrm{tur2}}-1)T_{L1}-E_{R2}T_{L3}]-C_{wf}T_{L1}[E_{R1}\eta_{\mathrm{com2}}(E_{R2}+\eta_{\mathrm{tur2}}-1)+E_{R1}(\eta_{\mathrm{tur2}}-1)(x_a-1)-\eta_{\mathrm{tur2}}(\eta_{\mathrm{com2}}+x_a)+\eta_{\mathrm{tur2}}+x_a-1]\}-[E_{R1}(2E_{R2}-1)-E_{R2}]C_{L2min}C_{wf}E_{L2}T_{L3}(x_a+\eta_{\mathrm{com2}}-1)\}+C_{L1min}E_{L1}\eta_{\mathrm{tur2}}T_{L1}(E_{R1}-1)(\eta_{\mathrm{com2}}+x_a-1)(C_{wf}-C_{L2min}E_{L2})\}/\{(\eta_{\mathrm{com2}}+x_a-1)x_a y_a(C_{wf}-C_{L1min}E_{L1})[E_{R1}(2E_{R2}-1)-E_{R2}]\}-C_{H1min}E_{H1}(E_{R2}-1)T_{H1}[(\eta_{\mathrm{tur1}}-1)xy-\eta_{t1}]\{(2E_{R1}-1)C_{L2min}E_{L2}(\eta_{\mathrm{com2}}+x_a-1)(\eta_{\mathrm{tur2}}+x_a y_a-x_a y_a\eta_{\mathrm{tur2}})+C_{wf}x_a y_a[E_{R1}\eta_{\mathrm{com2}}(2\eta_{\mathrm{tur2}}-1)+2E_{R1}(\eta_{\mathrm{tur2}}-1)(x_a-1)-(\eta_{\mathrm{com2}}+x_a)\eta_{\mathrm{tur2}}+\eta_{\mathrm{tur2}}+x_a-1]-C_{wf}\eta_{\mathrm{tur2}}(2E_{R1}-1)(x_a+\eta_{\mathrm{com2}}-1)\}\}/\{C_{wf}xyx_a y_a[E_{R1}(2E_{R2}-1)-E_{R2}](\eta_{\mathrm{com2}}+x_a-1)\}$$

$$a_3=\{a_1E_{R1}[E_{R1}(2E_{R2}-1)-E_{R2}]\{C_{H1min}E_{H1}(E_{R2}-1)[(\eta_{\mathrm{tur1}}-1)xy-\eta_{\mathrm{tur1}}]\{C_{L1min}C_{L2min}E_{L1}E_{L2}(\eta_{\mathrm{com1}}+x-1)\{x_a y_a[E_{R1}(\eta_{\mathrm{tur2}}-1)T_{L1}-E_{R1}T_{L3}+T_{L3}]-E_{R1}\eta_{\mathrm{tur2}}T_{L1}\}+C_{L1min}C_{wf}E_{L1}E_{R1}T_{L1}(\eta_{\mathrm{com1}}+x-1)(\eta_{\mathrm{tur2}}+x_a y_a-x_a\eta_{\mathrm{tur2}}y_a)+C_{L2min}C_{wf}E_{L2}\{E_{R1}\eta_{\mathrm{com1}}\eta_{\mathrm{tur2}}T_{H1}+x_a y_a[E_{R1}\eta_{\mathrm{com1}}(T_{H1}+T_{L3}-\eta_{\mathrm{tur2}}T_{H1})+E_{R1}T_{L3}(x-1)-T_{L3}(\eta_{\mathrm{com1}}+x)+T_{L3}]\}/C_{wf}+C_{wf}^2E_{R1}\eta_{\mathrm{com1}}T_{H1}[(\eta_{\mathrm{tur2}}-1)x_a y_a-\eta_{\mathrm{tur2}}]\}+C_{L1min}E_{L1}(\eta_{\mathrm{com1}}+x-1)[(\eta_{\mathrm{tur1}}-1)xy-\eta_{\mathrm{tur1}}](E_{R2}-1)\{[(C_{wf}-C_{L2min}E_{L2})E_{R1}T_{L1}(\eta_{\mathrm{tur2}}-1)+C_{L2min}E_{L2}(E_{R1}-1)T_{L3}]x_a y_a+E_{R1}\eta_{\mathrm{tur2}}T_{L1}(C_{L2min}E_{L2}-C_{wf})\}-C_{L2min}C_{wf}E_{L2}T_{L3}x_a y_a\{(E_{R1}-1)(E_{R2}-1)\eta_{\mathrm{tur1}}(\eta_{\mathrm{com1}}+x-1)(xy-1)+xy[E_{R1}(E_{R2}+\eta_{\mathrm{com1}}+x-1-2E_{R2}\eta_{\mathrm{com1}}-E_{R2}x)+E_{R2}(\eta_{\mathrm{com1}}+x-1)-x+1]\}\}/[xx_a yy_a(\eta_{\mathrm{com1}}+x-1)]-a_1a_2E_{R2}(E_{R1}-1)(E_{R1}+E_{R2}-2E_{R1}E_{R2})\{C_{H1min}E_{H1}E_{R1}(C_{wf}-C_{L1min}E_{L1})(E_{R2}-1)[(\eta_{\mathrm{tur1}}-1)xy-\eta_{\mathrm{tur1}}]/(C_{wf}E_{R2}xy)+E_{R1}\eta_{\mathrm{tur1}}(E_{R2}-1)(C_{wf}-C_{L1min}E_{L1})/(E_{R2}xy)-E_{R1}(E_{R2}-1)(\eta_{\mathrm{tur1}}-1)(C_{wf}-C_{L1min}E_{L1})/E_{R2}+C_{wf}\eta_{\mathrm{com1}}(E_{R1}-1)/(\eta_{\mathrm{com1}}+x-1)\}+E_{R2}(E_{R1}-1)(-2E_{R1}E_{R2}+E_{R1}+E_{R2})\{-C_{H1min}E_{H1}E_{R1}(E_{R2}-1)T_{H1}(C_{wf}-C_{L1min}E_{L1})[(\eta_{\mathrm{tur1}}-1)xy-\eta_{\mathrm{tur1}}]/(C_{wf}E_{R2}xy)-C_{L1min}E_{L1}(E_{R1}-1)T_{L1}\}\}/[(C_{wf}-C_{L1min}E_{L1})(E_{R1}+E_{R2}-2E_{R1}E_{R2})^2]$$

$$a_4=\{\eta_{\mathrm{com2}}\{\{a_1a_2(E_{R1}-1)\{\{C_{H1min}E_{H1}(E_{R1}-1)(E_{R2}-1)[(\eta_{\mathrm{tur1}}-1)xy-\eta_{\mathrm{tur1}}]\}/(C_{wf}xy)+[(E_{R1}E_{R2}-1)C_{wf}\eta_{\mathrm{com1}}]/[(x+\eta_{\mathrm{com1}}-1)(C_{wf}-C_{L1min}E_{L1})]-[(E_{R1}-1)(E_{R2}-1)(xy-1)\eta_{\mathrm{tur1}}]/(xy)+E_{R1}E_{R2}-E_{R1}-E_{R2}+1\}\}/(E_{R1}+E_{R2}-2E_{R1}E_{R2})\{E_{R1}\{\{C_{H1min}E_{H1}E_{R1}T_{H1}(E_{R2}-1)[(\eta_{\mathrm{tur1}}-1)xy-\eta_{\mathrm{tur1}}]\}/(C_{wf}xy)+[C_{L1min}E_{L1}E_{R2}T_{L1}(E_{R1}-1)]/(C_{wf}-C_{L1min}E_{L1})\}\}/(E_{R1}+E_{R2}-2E_{R1}E_{R2})-\{\{C_{H1min}E_{H1}E_{R1}(E_{R2}-1)T_{H1}(C_{wf}-C_{L1min}E_{L1})[(\eta_{\mathrm{tur1}}-1)xy-\eta_{\mathrm{tur1}}]\}/(C_{wf}E_{R2}xy)+E_{L1}T_{L1}C_{L1min}(E_{R1}-1)\}/[(E_{R1}+E_{R2}-2E_{R1}E_{R2})(C_{wf}-C_{L1min}E_{L1})]+\{C_{H1min}E_{H1}(E_{R2}-1)T_{H1}[(\eta_{\mathrm{tur1}}-1)\,xy-\eta_{\mathrm{tur1}}]\}/(C_{wf}E_{R2}xy)\}\}/[(E_{R1}-1)(\eta_{\mathrm{com2}}+x_a-1)]$$

$$a_5=[1/(C_{wf}E_{R2}xx_a yy_a)][(\eta_{\mathrm{tur2}}-1)x_a y_a-\eta_{\mathrm{tur2}}]\{-\{\{a_1a_2E_{R2}\{C_{H1min}E_{H1}(2E_{R1}-1)(E_{R2}-1)[(\eta_{\mathrm{tur1}}-1)xy-\eta_{\mathrm{tur1}}]+[xy\eta_{\mathrm{com1}}(E_{R1}-1)C_{wf}^2]/[(\eta_{\mathrm{com1}}+x-1)(C_{wf}-C_{L1min}E_{L1})]-C_{wf}(2E_{R1}-1)(E_{R2}-1)[(\eta_{\mathrm{tur1}}-1)xy-\eta_{\mathrm{tur1}}]\}\}/(E_{R1}+E_{R2}-2E_{R1}E_{R2})\}+\{C_{H1min}E_{H1}E_{R1}T_{H1}(E_{R2}-1)(C_{wf}-C_{L1min}E_{L1})[(\eta_{\mathrm{tur1}}-1)xy-\eta_{\mathrm{tur1}}]+(E_{R1}-1)C_{L1min}C_{wf}E_{L1}E_{R2}T_{L1}xy\}/\{[E_{R1}(2E_{R2}-1)-E_{R2}](C_{wf}-C_{L1min}E_{L1})\}+C_{H1min}E_{H1}(E_{R2}-1)T_{H1}[(\eta_{\mathrm{tur1}}-1)xy-\eta_{\mathrm{tur1}}]\}$$

$$b_1=\{-C_{L2min}E_{L2}\{C_{wf}x(2E_{R1}-1)(E_{R2}-1)(C_{H1min}E_{H1}+C_{L1min}E_{L1})-C_{H1min}C_{L1min}E_{H1}E_{L1}x(2E_{R1}-1)(E_{R2}-1)+C_{wf}^2\{x(2E_{R1}-1)(E_{R2}-1)(xy-1)+xy[E_{R1}(2x-1-2E_{R2}x)+E_{R2}x-x+1]\}\}/\{[E_{R1}(2E_{R2}-1)-E_{R2}]C_{wf}x^2y(C_{wf}-C_{L1min}E_{L1})\}+\{C_{H1min}E_{H1}(E_{R2}-1)\{[x_a-1+x_a(2E_{R1}-1)(x_a y_a-1)-E_{R1}(2x_a-1)]x_a y_a\}/(xy)+C_{wf}^2\{x_a y_a[(x_a-E_{R2})E_{R1}-x_a+1]-x_a(E_{R1}-1)(x_a y_a-1)\}/[x(C_{wf}-C_{L1min}E_{L1})]-C_{wf}(E_{R2}-1)\{x_a(2E_{R1}-1)(x_a y_a-1)+x_a y_a[x_a-1-E_{R1}(2x_a-1)]\}/(xy)\}/[x_a(E_{R1}+E_{R2}-2E_{R1}E_{R2})]\}/(x_a y_a)$$

$$b_2=\{\{x_a y_a\{C_{L1min}E_{L1}\{C_{L2min}E_{L2}x_a[E_{R1}T_{L3}(2E_{R2}-1)-E_{R2}T_{L3}]-C_{wf}T_{L1}[E_{R1}E_{R2}-(1+x_a)+x_a]\}-C_{L2min}C_{wf}E_{L2}T_{L3}x_a[E_{R1}(2E_{R2}-1)-E_{R2}]\}+C_{L1min}E_{L1}T_{L1}x_a(E_{R1}-1)(C_{wf}-C_{L2min}E_{L2})\}/\{x_a^2y_a(C_{wf}-C_{L1min}E_{L1})[E_{R1}(2E_{R2}-1)-E_{R2}]\}+C_{H1min}E_{H1}T_{H1}(E_{R2}-1)\{(2E_{R1}-1)C_{L2min}E_{L2}x_a+C_{wf}x_a y_a[E_{R1}-(1+x_a)+x_a]-(2E_{R1}-1)C_{wf}x_a\}\}/\{C_{wf}xyx_a^2y_a[E_{R1}(2E_{R2}-1)-E_{R2}]\}$$

$$\begin{aligned}&b_3=\{b_1E_{R1}[E_{R1}(2E_{R2}-1)-E_{R2}]\{-C_{H1min}E_{H1}(E_{R2}-1)\{C_{L1min}C_{L2min}E_{L1}E_{L2}x[x_ay_a(T_{L3}-E_{R1}T_{L3})-E_{R1}T_{L1}]+C_{wf}E_{L1}\\&C_{L1min}E_{R1}T_{L1}x+C_{L2min}C_{wf}E_{L2}\{E_{R1}T_{H1}+x_ay_a[xE_{R1}T_{L3}-T_{L3}(1+x)+T_{L3}]\}/C_{wf}-C_{wf}^2E_{R1}T_{H1}\}-xC_{L1min}E_{L1}(E_{R2}-1)[x_a\\&E_{L2}C_{L2min}T_{L3}y_a(E_{R1}-1)+E_{R1}T_{L1}(C_{L2min}E_{L2}-C_{wf})]-C_{L2min}C_{wf}E_{L2}T_{L3}x_ay_a\{x(E_{R1}-1)(E_{R2}-1)(xy-1)+xy[E_{R1}(E_{R2}\\&+x-2E_{R2}-E_{R2}x)+E_{R2}x-x+1]\}\}/(x^2x_ayy_a)-b_1b_2E_{R2}(E_{R1}-1)(E_{R1}+E_{R2}-2E_{R1}E_{R2})\{-C_{H1min}E_{H1}E_{R1}(C_{wf}-E_{L1}\\&C_{L1min})(E_{R2}-1)/(C_{wf}E_{R2}xy)+E_{R1}(C_{wf}-C_{L1min}E_{L1})(E_{R2}-1)/(E_{R2}xy)+C_{wf}(E_{R1}-1)/x\}+E_{R2}(E_{R1}-1)(E_{R1}+E_{R2}\\&-2E_{R1}E_{R2})\{C_{H1min}E_{H1}E_{R1}T_{H1}(C_{wf}-C_{L1min}E_{L1})(E_{R2}-1)/(C_{wf}E_{R2}xy)-C_{L1min}E_{L1}(E_{R1}-1)T_{L1}\}\}/[(C_{wf}-C_{L1min}E_{L1})(\\&E_{R1}+E_{R2}-2E_{R1}E_{R2})^2]\end{aligned}$$

$$\begin{aligned}&b_4=\{\{\{b_1b_2(E_{R1}-1)\{[-C_{H1min}E_{H1}(E_{R1}-1)(E_{R2}-1)]/(C_{wf}xy)+[(E_{R1}E_{R2}-1)C_{wf}]/[x(C_{wf}-C_{L1min}E_{L1})]-[(E_{R1}-1)\\&(E_{R2}-1)(xy-1)]/(xy)+E_{R1}E_{R2}-E_{R1}-E_{R2}+1\}\}/(E_{R2}+E_{R1}-2E_{R1}E_{R2})+\{E_{R1}\{[-C_{H1min}E_{H1}E_{R1}(E_{R2}-1)T_{H1}]/(\\&C_{wf}xy)+[C_{L1min}E_{L1}E_{R2}T_{L1}(E_{R1}-1)]/(C_{wf}-C_{L1min}E_{L1})/(E_{R1}+E_{R2}-2E_{R1}E_{R2})-\{[-E_{H1}C_{H1min}E_{R1}T_{H1}(E_{R2}-1)(C_{wf}\\&-C_{L1min}E_{L1})]/(C_{wf}E_{R2}xy)+C_{L1min}E_{L1}T_{L1}(E_{R1}-1)\}/[(C_{wf}-C_{L1min}E_{L1})(E_{R1}+E_{R2}-2E_{R1}E_{R2})+[-C_{H1min}E_{H1}(E_{R2}-1)\\&T_{H1}]/(C_{wf}E_{R2}xy)\}\}/[x_a(E_{R1}-1)]\end{aligned}$$

$$\begin{aligned}&b_5=[-1/(C_{wf}E_{R2}xx_ayy_a)]\{-\{\{b_1b_2E_{R2}\{-C_{H1min}E_{H1}(2E_{R1}-1)(E_{R2}-1)+[C_{wf}^2xy(E_{R1}-1)]/[-(C_{wf}-C_{L1min}E_{L1})]+\\&C_{wf}(2E_{R1}-1)(E_{R2}-1)\}\}/(-2E_{R1}E_{R2}+E_{R1}+E_{R2})\}+\{-C_{H1min}E_{H1}E_{R1}T_{H1}(E_{R2}-1)(C_{wf}-C_{L1min}E_{L1})+C_{L1min}C_{wf}E_{L1}\\&E_{R2}T_{L1}xy(E_{R1}-1)\}/\{[E_{R1}(2E_{R2}-1)-E_{R2}](C_{wf}-C_{L1min}E_{L1})\}-C_{H1min}E_{H1}T_{H1}(E_{R2}-1)\end{aligned}$$

$$\begin{aligned}&c_1=\{C_{wf}E_{L2}[(\eta_{tur2}-1)x_ay_a-\eta_{tur2}]\{-C_{wf}(2E_{R1}-1)(E_{R2}-1)(\eta_{com1}+x-1)[(\eta_{tur1}-1)xy-\eta_{tur1}](C_{wf}E_{H1}+C_{wf}E_{L1})+\\&E_{H1}C_{wf}^2E_{L1}(2E_{R1}-1)(E_{R2}-1)(\eta_{com1}+x-1)[(\eta_{tur1}-1)xy-\eta_{tur1}]+C_{wf}^2\{\eta_{tur1}(2E_{R1}-1)(E_{R2}-1)(\eta_{com1}+x-1)(xy-1)+\\&xy\{E_{R1}[\eta_{com1}+2x-2-2E_{R2}(\eta_{com1}+x-1)]+E_{R2}(\eta_{com1}+x-1)-x+1\}\}\}/\{(\eta_{com1}+x-1)[E_{R1}(2E_{R2}-1)-E_{R2}]C_{wf}^2\\&xy(1-E_{L1})\}+\{-C_{wf}E_{H1}(E_{R2}-1)[(\eta_{tur1}-1)xy-\eta_{tur1}]\{x_ay_a[x_a-1-E_{R1}(\eta_{com2}+2x_a-2)]+\eta_{tur2}(2E_{R1}-1)(\eta_{com2}+x_a\\&-1)(x_ay_a-1)\}/(xy)+C_{wf}^2\eta_{com1}\{x_ay_a[(\eta_{com2}+x_a-1-E_{R2}\eta_{com2})E_{R1}-x_a+1]-\eta_{tur2}(E_{R1}-1)(\eta_{com2}+x_a-1)(x_ay_a-1\\&)\}/[C_{wf}(\eta_{com1}+x-1)(1-E_{L1})]+C_{wf}(E_{R2}-1)[(\eta_{tur1}-1)xy-\eta_{tur1}]\{(2E_{R1}-1)(\eta_{com2}+x_a-1)(x_ay_a-1)\eta_{tur2}+x_ay_a[x_a\\&-1-E_{R1}(\eta_{com2}+2x_a-2)]\}/(xy)\}/[(E_{R1}+E_{R2}-2E_{R1}E_{R2})(\eta_{com2}+x_a-1)]\}/(x_ay_a)\end{aligned}$$

$$\begin{aligned}&c_2=\{\{x_ay_a\{C_{wf}E_{L1}\{C_{wf}E_{L2}(\eta_{com2}+x_a-1)[E_{R1}T_{L3}(2E_{R2}-1)+(E_{R1}-1)(\eta_{tur2}-1)T_{L1}-E_{R2}T_{L3}]-C_{wf}T_{L1}\{(E_{R2}+\eta_{tur2}\\&-1)E_{R1}\eta_{com2}+E_{R1}(\eta_{tur2}-1)(x_a-1)-\eta_{tur2}(\eta_{com2}+x_a)+\eta_{tur2}+x_a-1\}\}-C_{wf}^2E_{L2}T_{L3}[E_{R1}(2E_{R2}-1)-E_{R2}](\eta_{com2}+x_a-\\&1)\}+C_{wf}^2E_{L1}\eta_{tur2}T_{L1}(E_{R1}-1)(\eta_{com2}+x_a-1)(1-E_{L2})\}/\{(\eta_{com2}+x_a-1)x_ay_aC_{wf}(1-E_{L1})[E_{R1}(2E_{R2}-1)-E_{R2}]\}-C_{wf}\\&E_{H1}(E_{R2}-1)T_{H1}[(\eta_{tur1}-1)xy-\eta_{tur1}]\{C_{wf}E_{L2}(2E_{R1}-1)(\eta_{com2}+x_a-1)(\eta_{tur2}+x_ay_a-x_a\eta_{tur2}y_a)+C_{wf}x_ay_a[E_{R1}\eta_{com2}(2\\&\eta_{tur2}-1)+2E_{R1}(\eta_{tur2}-1)(x_a-1)-(\eta_{com2}+x_a)\eta_{tur2}+\eta_{tur2}+x_a-1]-C_{wf}\eta_{tur2}(2E_{R1}-1)(\eta_{com2}+x_a-1)\}\}/\{(\eta_{com2}+x_a\\&-1)C_{wf}xyx_ay_a[E_{R1}(2E_{R2}-1)-E_{R2}]\}\end{aligned}$$

$$\begin{aligned}&c_3=\{c_1E_{R1}[E_{R1}(2E_{R2}-1)-E_{R2}]\{C_{wf}E_{H1}(E_{R2}-1)[(\eta_{tur1}-1)xy-\eta_{tur1}]\{C_{wf}^2E_{L1}E_{L2}(\eta_{com1}+x-1)\{E_{R1}\eta_{tur2}T_{L1}-x_ay_a[\\&E_{R1}T_{L1}(\eta_{tur2}-1)-E_{R1}T_{L3}+T_{L3}]\}+C_{wf}^2E_{L1}E_{R1}T_{L1}(\eta_{com1}+x-1)(\eta_{tur2}+x_ay_a-x_a\eta_{tur2}y_a)+C_{wf}E_{L2}\{E_{R1}\eta_{com1}\eta_{tur2}T_{H1}+x_a\\&y_a[T_{L3}+E_{R1}\eta_{com1}(T_{H1}+T_{L3}-\eta_{tur2}T_{H1})+E_{R1}T_{L3}(x-1)-T_{L3}(\eta_{com1}+x)]\}+C_{wf}^2E_{R1}\eta_{com1}T_{H1}[(\eta_{tur2}-1)x_ay_a-\eta_{tur2}]\}+C_{wf}\\&(\eta_{com1}+x-1)E_{L1}[(\eta_{tur1}-1)xy-\eta_{tur1}](E_{R2}-1)\{x_ay_a[C_{wf}E_{R1}T_{L1}(1-E_{L2})(\eta_{tur2}-1)+C_{wf}E_{L2}(E_{R1}-1)T_{L3}]+E_{R1}\eta_{tur2}T_{L1}(\\&C_{wf}E_{L2}-C_{wf})\}-C_{wf}^2E_{L2}T_{L3}x_ay_a\{(\eta_{tur1}E_{R1}-1)(E_{R2}-1)(\eta_{com1}+x-1)(xy-1)+xy[E_{R1}(E_{R2}+\eta_{com1}+x-1-2\eta_{com1}E_{R2}\\&-E_{R2}x)+E_{R2}(\eta_{com1}+x-1)-x+1]\}\}/[xx_ayy_a(\eta_{com1}+x-1)]-c_1c_2E_{R2}(E_{R1}-1)(E_{R1}+E_{R2}-2E_{R1}E_{R2})\{C_{wf}^2(1-E_{L1}\\&)(E_{R2}-1)E_{H1}E_{R1}[(\eta_{tur1}-1)xy-\eta_{tur1}]/(C_{wf}E_{R2}xy)+E_{R1}C_{wf}(E_{R2}-1)(1-E_{L1})\eta_{tur1}/(E_{R2}xy)-C_{wf}(\eta_{tur1}-1)(1-E_{L1})\\&(E_{R2}-1)E_{R1}/E_{R2}+C_{wf}\eta_{com1}(E_{R1}-1)/(\eta_{com1}+x-1)\}+E_{R2}(E_{R1}-1)(E_{R1}+E_{R2}-2E_{R1}E_{R2})\{-C_{wf}^2E_{H1}E_{R1}T_{H1}(E_{R2}-\\&1)(1-E_{L1})[(\eta_{tur1}-1)xy-\eta_{tur1}]/(C_{wf}E_{R2}xy)-C_{wf}E_{L1}T_{L1}(E_{R1}-1)\}\}/[C_{wf}(1-E_{L1})(E_{R1}+E_{R2}-2E_{R1}E_{R2})^2]\end{aligned}$$

$$\begin{aligned}&c_4=\{\eta_{com2}\{\{c_1c_2(E_{R1}-1)\{E_{H1}(E_{R1}-1)(E_{R2}-1)[(\eta_{tur1}-1)xy-\eta_{tur1}]/(xy)+\eta_{com1}(E_{R1}E_{R2}-1)/[(\eta_{com1}+x-1)(1-E_{L1}\\&)]-\eta_{tur1}(E_{R1}-1)(E_{R2}-1)(xy-1)/(xy)+E_{R1}E_{R2}-E_{R1}-E_{R2}+1\}\}/(E_{R1}+E_{R2}-2E_{R1}E_{R2})+\{E_{R1}\{(E_{R2}-1)E_{H1}E_{R1}\\&T_{H1}[(\eta_{tur1}-1)xy-\eta_{tur1}]/(xy)+[E_{L1}E_{R2}T_{L1}(E_{R1}-1)]/(1-E_{L1})\}\}/(E_{R1}+E_{R2}-2E_{R1}E_{R2})-\{\{C_{wf}(E_{R2}-1)(1-E_{L1})C_{w}\\&E_{H1}E_{R1}T_{H1}[(\eta_{tur1}-1)xy-\eta_{tur1}]\}/(C_{wf}E_{R2}xy)+C_{wf}E_{L1}T_{L1}(E_{R1}-1)\}/[C_{wf}(E_{R1}+E_{R2}-2E_{R1}E_{R2})(1-E_{L1})]+\{C_{wf}E_{H1}(\\&E_{R2}-1)T_{H1}[(\eta_{tur1}-1)xy-\eta_{tur1}]\}/(C_{wf}E_{R2}xy)\}\}/[(E_{R1}-1)(\eta_{com2}+x_a-1)]\end{aligned}$$

$$\begin{aligned}&c_5=[1/(C_{wf}E_{R2}xx_ayy_a)][(\eta_{tur2}-1)x_ay_a-\eta_{tur2}]\{-\{\{c_1c_2E_{R2}\{C_{wf}E_{H1}(2E_{R1}-1)(E_{R2}-1)[(\eta_{tur1}-1)xy-\eta_{tur1}]+C_{wf}xy\\&\eta_{com1}(E_{R1}-1)/[(\eta_{com1}+x-1)(1-E_{L1})]-C_{wf}(2E_{R1}-1)(E_{R2}-1)[(\eta_{tur1}-1)xy-\eta_{tur1}]\}\}/(E_{R1}+E_{R2}-2E_{R1}E_{R2})\}+\{\\&C_{wf}E_{H1}E_{R1}T_{H1}(E_{R2}-1)(1-E_{L1})[(\eta_{tur1}-1)xy-\eta_{tur1}]+C_{wf}E_{L1}E_{R2}T_{L1}xy(E_{R1}-1)\}/\{[E_{R1}(2E_{R2}-1)-E_{R2}](1-E_{L1})\}+\\&C_{wf}E_{H1}T_{H1}(E_{R2}-1)[(\eta_{tur1}-1)xy-\eta_{tur1}]\}\end{aligned}$$

$$d_1=\{-C_{wf}E_{L2}\{C_{wf}^2x(2E_{R1}-1)(E_{R2}-1)(E_{H1}+E_{L1})-C_{wf}^2E_{H1}E_{L1}x(2E_{R1}-1)(E_{R2}-1)+C_{wf}^2\{x(2E_{R1}-1)(E_{R2}-1)(xy-1)+xy\{E_{R1}[2x-1-2E_{R2}x]+E_{R2}x-x+1\}\}\}/\{C_{wf}^2x^2y(1-E_{L1})[E_{R1}(2E_{R2}-1)-E_{R2}]\}+\{C_{wf}E_{H1}(E_{R2}-1)\{x_ay_a[-E_{R1}(2x_a-1)+x_a-1+x_a(2E_{R1}-1)(x_ay_a-1)]\}/(xy)+C_{wf}\{x_ay_a[(x_a-E_{R2})E_{R1}-x_a+1]-x_a(E_{R1}-1)(x_ay_a-1)\}/[x(1-E_{L1})]-C_{wf}(E_{R2}-1)\{x_a(2E_{R1}-1)(x_ay_a-1)+x_ay_a[x_a-1-E_{R1}(2x_a-1)]\}/(xy)\}/[x_a(E_{R1}+E_{R2}-2E_{R1}E_{R2})]\}/(x_ay_a)$$

$$d_2=\{\{x_ay_a\{C_{wf}^2E_{L1}\{E_{L2}x_a[E_{R1}T_{L3}(2E_{R2}-1)-E_{R2}T_{L3}]-T_{L1}(E_{R1}E_{R2}-1)\}-C_{wf}^2E_{L2}T_{L3}x_a[E_{R1}(2E_{R2}-1)-E_{R2}]\}+C_{wf}^2E_{L1}T_{L1}x_a(E_{R1}-1)(1-E_{L2})/\{C_{wf}x_a^2y_a(1-E_{L1})[E_{R1}(2E_{R2}-1)-E_{R2}]\}+C_{wf}^2E_{H1}T_{H1}(E_{R2}-1)\{(2E_{R1}-1)E_{L2}x_a+x_ay_a(E_{R1}-1)-x_a(2E_{R1}-1)\}\}/\{C_{wf}xyx_a^2y_a[E_{R1}(2E_{R2}-1)-E_{R2}]\}$$

$$d_3=\{d_1E_{R1}[E_{R1}(2E_{R2}-1)-E_{R2}]\{-C_{wf}E_{H1}(E_{R2}-1)\{C_{wf}^2E_{L1}E_{L2}x[x_ay_aT_{L3}(1-E_{R1})-E_{R1}T_{L1}]+xC_{wf}^2E_{L1}E_{R1}T_{L1}+C_{wf}E_{L2}\{E_{R1}T_{H1}+x_ay_a[E_{R1}T_{L3}+E_{R1}T_{L3}(x-1)-T_{L3}x]\}-C_{wf}^2E_{R1}T_{H1}\}-\{E_{L2}T_{L3}x_ay_a(E_{R1}-1)+(E_{L2}-1)E_{R1}T_{L1}\}C_{wf}^2xE_{L1}(E_{R2}-1)-C_{wf}^2E_{L2}T_{L3}x_ay_a\{xy[E_{R1}(E_{R2}+x-2E_{R2}-E_{R2}x)+E_{R2}x-x+1]+x(E_{R1}-1)(E_{R2}-1)(xy-1)\}\}/(x^2x_ayy_a)-d_1d_2E_{R2}(E_{R1}-1)(E_{R1}+E_{R2}-2E_{R1}E_{R2})\{-C_{wf}^2(1-E_{L1})(E_{R2}-1)E_{H1}E_{R1}/(C_{wf}E_{R2}xy)+C_{wf}E_{R1}(1-E_{L1})(E_{R2}-1)/(E_{R2}xy)+C_{wf}(E_{R1}-1)/x\}+(E_{R1}+E_{R2}-2E_{R1}E_{R2})E_{R2}(E_{R1}-1)\{C_{wf}^2E_{H1}E_{R1}T_{H1}(1-E_{L1})(E_{R2}-1)/(C_{wf}E_{R2}xy)-C_{wf}E_{L1}(E_{R1}-1)T_{L1}\}/[(C_{wf}-C_{wf}E_{L1})(E_{R1}+E_{R2}-2E_{R1}E_{R2})^2]$$

$$d_4=\{\{\{d_1d_2(E_{R1}-1)\{-E_{H1}(E_{R1}-1)(E_{R2}-1)/(xy)+(E_{R1}E_{R2}-1)/[x(1-E_{L1})]-(E_{R1}-1)(E_{R2}-1)(xy-1)/(xy)+E_{R1}E_{R2}-E_{R1}-E_{R2}+1\}\}/(E_{R2}+E_{R1}-2E_{R1}E_{R2})+\{E_{R1}\{-E_{H1}E_{R1}(E_{R2}-1)T_{H1}/(xy)+E_{L1}E_{R2}T_{L1}(E_{R1}-1)/(1-E_{L1})\}\}/(-2E_{R1}E_{R2}+E_{R1}+E_{R2})-\{-E_{H1}E_{R1}T_{H1}(E_{R2}-1)(1-E_{L1})/(E_{R2}xy)+E_{L1}T_{L1}(E_{R1}-1)\}/[(1-E_{L1})(E_{R1}+E_{R2}-2E_{R1}E_{R2})]-E_{H1}T_{H1}(E_{R2}-1)/(E_{R2}xy)\}\}/[x_a(E_{R1}-1)]$$

$$d_5=[-1/(C_{wf}E_{R2}xx_ayy_a)]\{-\{\{d_1d_2E_{R2}\{-C_{wf}E_{H1}(2E_{R1}-1)(E_{R2}-1)-C_{wf}xy(E_{R1}-1)/(1-E_{L1})+C_{wf}(2E_{R1}-1)(E_{R2}-1)\}\}/(E_{R1}+E_{R2}-2E_{R1}E_{R2})\}+\{C_{wf}^2E_{L1}E_{R2}T_{L1}xy(E_{R1}-1)-C_{wf}^2E_{H1}E_{R1}(E_{R2}-1)(1-E_{L1})T_{H1}\}/\{C_{wf}(1-E_{L1})[E_{R1}(2E_{R2}-1)-E_{R2}]\}-C_{wf}E_{H1}T_{H1}(E_{R2}-1)\}$$

$$e=\{-(\eta_{\mathrm{com1}}+x-1)\{C_{H1min}E_{H1}(C_{wf}-C_{L1min}E_{L1})T_{H1}[(\eta_{\mathrm{tur1}}-1)xy-\eta_{\mathrm{tur1}}]-C_{L1min}C_{wf}E_{L1}T_{L1}xy\}\}/\{C_{H1min}C_{L1min}E_{H1}E_{L1}(\eta_{\mathrm{com1}}+x-1)[(\eta_{\mathrm{tur1}}-1)xy-\eta_{\mathrm{tur1}}]+C_{wf}^2[(1-x)xy+\eta_{\mathrm{tur1}}(\eta_{\mathrm{com1}}+x-1)(xy-1)]-C_{wf}(C_{H1min}E_{H1}+E_LC_{L1min})(\eta_{\mathrm{com1}}+x-1)[(\eta_{\mathrm{tur1}}-1)xy-\eta_{\mathrm{tur1}}]\}$$

References

1. Invernizzi, C.M. Prospects of mixtures as working fluids in real-gas Brayton cycles. *Energies* **2017**, *10*, 1649.
2. Wang, J.P.; Wang, J.; Lund, P.D.; Zhu, H.X. Thermal performance analysis of a direct-heated recompression supercritical carbon dioxide Brayton cycle using solar concentrators. *Energies* **2019**, *12*, 4358.
3. Jaszczur, M.; Dudek, M.; Kolenda, Z. Thermodynamic analysis of advanced gas turbine combined cycle integration with a high-temperature nuclear reactor and cogeneration unit. *Energies* **2020**, *13*, 400.
4. Vecchiarelli, J.; Kawall, J.G.; Wallace, J.S. Analysis of a concept for increasing the efficiency of a Brayton cycle via isothermal heat addition. *Int. J. Energy Res.* **1997**, *21*, 113–127.
5. Göktun, S.; Yavuz, H. Thermal efficiency of a regenerative Brayton cycle with isothermal heat addition. *Energy Convers. Manag.* **1999**, *40*, 1259–1266.
6. Erbay, L.B.; Göktun, S.; Yavuz, H. Optimal design of the regenerative gas turbine engine with isothermal heat addition. *Appl. Energy* **2001**, *68*, 249–264.
7. Jubeh, N.M. Exergy analysis and second law efficiency of a regenerative Brayton cycle with isothermal heat addition. *Entropy* **2005**, *7*, 172–187.
8. El-Maksound, R.M.A. Binary Brayton cycle with two isothermal processes. E*nergy Convers. Manag.* **2013**, *73*, 303–308.
9. Qi, W.; Wang, W.H.; Chen, L.G. Exergy analysis and optimization for binary Brayton cycle with two isothermal heat additions. *Therm. Turbine* **2017**, *46*, 76–81 (In Chinese).
10. Andresen, B.; Salamon, P.; Barry, R.S. Thermodynamics in finite time. *Phys. Today* **1987**, *37*, 62–70.
11. Chen, L.G.; Li, J. Thermodynamic optimization theory for Two-Heat-Reservoir cycles; Science Press: Beijing, China, 2020.
12. Barranco-Jimenez, M.A.; Ramos-Gayosso, I.; Rosales, M.A.; Angulo-Brown, F. A proposal of ecologic taxes based on thermoeconomic performance of heat engine models. *Energies* **2009**, *2*, 1042–1056.

13. Chen, C.L.; Ho, C.E.; Yau, H.T. Performance analysis and optimization of a solar powered Stirling engine with heat transfer considerations. *Energies* **2012**, *5*, 3573–3585.
14. Gonca, G. Energy and exergy analyses of single and double reheat irreversible Rankine cycle. *Int. J. Exergy* **2015**, *18*, 402–422.
15. Han, Z.H.; Li, P.; Han, X.; Mei, Z.K.; Wang, Z. Thermo-economic performance analysis of a regenerative superheating organic Rankine cycle for waste heat recovery. *Energies* **2017**, *10*, 1593.
16. White, M.T.; Sayma, A.I. A generalised assessment of working fluids and radial turbines for non-recuperated subcritical organic Rankine cycles. *Energies* **2018**, *11*, 800.
17. Chen, W.J.; Feng, H.J.; Chen, L.G.; Xia, S.J. Optimal performance characteristics of subcritical simple irreversible organic Rankine cycle. *J. Therm. Sci.* **2018**, *27*, 555–562.
18. Vittorini, D.; Cipollone, R.; Carapellucci, R. Enhanced performances of ORC-based units for low grade waste heat recovery via evaporator layout optimization. *Energy Convers. Manag.* **2019**, *197*, 111874.
19. Koo, J.; Oh, S.R.; Choi, Y.U.; Jung, J.H.; Park, K. Optimization of an organic Rankine cycle system for an LNG-powered ship. *Energies* **2019**, *12*, 1933.
20. Wang, S.; Zhang, W.; Feng, Y.Q.; Wang, X.; Wang, Q.; Liu, Y.Z.; Wang, Y.; Yao, L. Entropy, entransy and exergy analysis of a dual-loop organic Rankine cycle (DORC) using mixture working fluids for engine waste heat recovery. *Energies* **2020**, *13*, 1301.
21. Feng, H.J.; Chen, W.J.; Chen, L.G.; Tang, W. Power and efficiency optimizations of an irreversible regenerative organic Rankine cycle. *Energy Convers. Manag.* **2020**, *220*, 113079.
22. Chen, L.G.; Ma K.; Feng, H.J.; Ge, Y.L. Optimal configuration of a gas expansion process in a piston-type cylinder with generalized convective heat transfer law. *Energies*, 2020, *13*, in press.
23. Chen, L.G.; Meng, F.K.; Sun, F.R. Thermodynamic analyses and optimizations for thermoelectric devices: the state of the arts. *Sci. China Technol. Sci.* **2016**, *59*, 442–455.
24. Chen, J.L.; Li, K.W.; Liu, C.W.; Li, M.; Lv, Y.C.; Jia, L.; Jiang, S.S. Enhanced efficiency of thermoelectric generator by optimizing mechanical and electrical structures. *Energies* **2017**, *10*, 1329.
25. Feng, Y.L.; Chen, L.G.; Meng, F.K.; Sun, F.R. Influences of external heat transfer and Thomson effect on performance of TEG-TEC combined thermoelectric device. *Sci. China Technol. Sci.* **2018**, *61*, 1600–1610.
26. Li, G.; Wang, Z.C.; Wang, F.; Wang, X.Z.; Li, S.B.; Xue, M.S. Experimental and numerical study on the effect of interfacial heat transfer on performance of thermoelectric generators. *Energies* **2019**, *12*, 3797.
27. Açıkkalp, E.; Chen, L.G.; Ahmadi, M.H. Comparative performance analyses of molten carbonate fuel cell-alkali metal thermal to electric converter and molten carbonate fuel cell –thermoelectric generator hybrid systems. *Energy Rep.* **2020**, *6*, 10–16.
28. Gonca, G. Exergetic and thermo-ecological performance analysis of a Gas-Mercury combined turbine system (GMCTS). *Energy Convers. Manag.* **2017**, *151*, 32–42.
29. Lin, J.; Zhang, Z.H.; Zhu, X.Y.; Meng, C.; Li, N.; Chen, J.C.; Zhao, Y.R. Performance evaluation and parametric optimization strategy of a thermocapacitive heat engine to harvest low-grade heat. *Energy Convers. Manag.* **2019**, *184*, 40–47.
30. Zhu, F.L.; Chen, L.G.; Wang, W.H. Thermodynamic analysis and optimization of irreversible Maisotsenko-Diesel cycle. *J. Therm. Sci.* **2019**, *28*, 659–668.
31. Dumitrascu, G.; Feidt, M.; Popescu, A.; Grigorean, S. Endoreversible trigeneration cycle design based on finite physical dimensions thermodynamics. *Energies* **2019**, *12*, 3165.
32. Wu, Z.X.; Chen, L.G.; Feng, H.J. Thermodynamic optimization for an endoreversible Dual-Miller cycle (DMC) with finite speed of piston. *Entropy* **2018**, *20*, 165.
33. You, J.; Chen, L.G.; Wu, Z.X.; Sun, F.R. Thermodynamic performance of Dual-Miller cycle (DMC) with polytropic processes based on power output, thermal efficiency and ecological function. *Sci. China Technol. Sci.* **2018**, *61*, 453–463.
34. Abedinnezhad, S.; Ahmadi, M.H.; Pourkiaei, S.M.; Pourfayaz, F.; Mosavi, A.; Feidt, M.; Shamshirband, S. Thermodynamic assessment and multi-objective optimization of performance of irreversible Dual-Miller cycle. *Energies* **2019**, *12*, 4000.
35. Ding, Z.M.; Ge, Y.L.; Chen, L.G.; Feng, H.J.; Xia, S.J. Optimal performance regions of Feynman's ratchet engine with different optimization criteria. *J. Non-Equilib. Thermodyn.* **2020**, *45*, 191–207.
36. Feng, H.J.; Qin, W.X.; Chen, L.G.; Cai, C.G.; Ge, Y.L.; Xia, S.J. Power output, thermal efficiency and exergy-based ecological performance optimizations of an irreversible KCS-34 coupled to variable temperature heat reservoirs. *Energy Convers. Manag.* **2020**, *205*, 112424.

37. Chen, L.G.; Sun, F.R.; Wu, C. Performance analysis of an irreversible Brayton heat engine. *J. Inst. Energy* **1997**, *70*, 2–8.
38. Sadatsakkak, S.A.; Ahmadi, M.H.; Ahmadi, M.A. Thermodynamic and thermo-economic analysis and optimization of an irreversible regenerative closed Brayton cycle. *Energy Convers. Manag.* **2015**, *94*, 124–129.
39. Naserian, M.M.; Farahat, S.; Sarhaddi, F. Finite time exergy analysis and multi-objective ecological optimization of a regenerative Brayton cycle considering the impact of flow rate variations. *Energy Convers. Manag.* **2015**, *103*, 790–800.
40. Jansen, E.; Bello-Ochende, T.; Meyer, J.P. Integrated solar thermal Brayton cycles with either one or two regenerative heat exchangers for maximum power output. *Energy* **2015**, *86*, 737–748.
41. Sánchez-Orgaz, S.; Medina, A.; Calvo Hernández, A. Thermodynamic model and optimization of a multi-step irreversible Brayton cycle. *Energy Convers. Manag.* **2010**, *51*, 2134–2143.
42. Sanchez-Orgaz, S.; Pedemonte, M.; Ezzatti, P.; Curto-Risso, P.L.; Medina, A.; Calvo Hernández, A. Multi-objective optimization of a multi-step solar-driven Brayton plant. *Energy Convers. Manag.* **2015**, *99*, 346–358.
43. Chen, L.G.; Feng, H.J.; Ge, Y.L. Power and efficiency optimization for open combined regenerative Brayton and inverse Brayton cycles with regeneration before the inverse cycle. *Entropy* **2020**, 22, 677.
44. Açıkkalp, E. Performance analysis of irreversible solid oxide fuel cell–Brayton heat engine with ecological based thermo-environmental criterion. *Energy Convers. Manag.* **2017**, *148*, 279–286.
45. Zhu, F.L.; Chen, L.G.; Wang, W.H. Thermodynamic analysis of an irreversible Maisotsenko reciprocating Brayton cycle. *Entropy* **2018**, *20*, 167.
46. Chen, L.G.; Shen, J.F.; Ge, Y.L.; Wu, Z.X.; Wang, W.H.; Zhu, F.L.; Feng, H.J. Power and efficiency optimization of open Maisotsenko-Brayton cycle and performance comparison with traditional open regenerated Brayton cycle. *Energy Convers. Manag.* **2020**, *217*, 113001.
47. Feng, H.J.; Tao, G.S.; Tang, C.Q.; Ge, Y.L.; Chen, L.G.; Xia, S.J. Exergoeconomic performance optimization for a regenerative gas turbine closed-cycle heat and power cogeneration plant. *Energy Rep.* **2019**, *5*, 1525–1531.
48. Chen, L.G.; Yang, B.; Feng, H.J.; Ge, Y.L.; Xia, S.J. Performance optimization of an open simple-cycle gas turbine combined cooling, heating and power plant driven by basic oxygen furnace gas in China's steelmaking plants. *Energy* **2020**, *203*, 117791.
49. Kaushik, S.C.; Tyagi, S.K.; Singhal, M.K. Parametric study of an irreversible regenerative Brayton cycle with isothermal heat addition. *Energy Convers. Manag.* **2003**, *44*, 2013–2025.
50. Tyagi, S.K.; Kaushik, S.C.; Tiwari, V. Ecological optimization and parametric study of an irreversible regenerative modified Brayton cycle with isothermal heat addition. *Entropy* **2003**, *5*, 377–390.
51. Tyagi, S.K.; Chen, J.C. Performance evaluation of an irreversible regenerative modified Brayton heat engine based on the thermoeconomic criterion. *Int. J. Power Energy Syst.* **2006**, *26*, 66–74.
52. Kumar, R.; Kaushik, S.C.; Kumar, R. Power optimization of an irreversible regenerative Brayton cycle with isothermal heat addition. *J. Therm. Eng.* **2015**, *1*, 279–286.
53. Tyagi, S.K.; Chen, J.; Kaushik, S.C. Optimum criteria based on the ecological function of an irreversible intercooled regenerative modified Brayton cycle. *Int. J. Exergy* **2005**, *2*, 90–107.
54. Tyagi, S.K.; Wang, S.; Kaushik, S.C. Irreversible modified complex Brayton cycle under maximum economic condition. *Indian J. Pure Appl. Phys.* **2006**, *44*, 592–601.
55. Tyagi, S.K.; Chen, J.; Kaushik, S.C.; Wu, C. Effects of intercooling on the performance of an irreversible regenerative modified Brayton cycle. *Int. J. Power Energy Syst.* **2007**, *27*, 256–264.
56. Tyagi, S.K.; Wang, S.; Park, S.R. Performance criteria on different pressure ratios of an irreversible modified complex Brayton cycle. *Indian J. Pure Appl. Phys.* **2008**, *46*, 565–574.
57. Wang, J.H.; Chen, L.G.; Ge, Y.L.; Sun, F.R. Power and power density analyzes of an endoreversible modified variable-temperature reservoir Brayton cycle with isothermal heat addition. *Int. J. Low-Carbon Technol.* **2016**, *11*, 42–53.
58. Wang, J.H.; Chen, L.G.; Ge, Y.L.; Sun, F.R. Ecological performance analysis of an endoreversible modified Brayton cycle. *Int. J. Sustain. Energy* **2014**, *33*, 619–634.
59. Tang, C.Q.; Chen, L.G.; Wang, W.H.; Feng, H.J.; Xia, S.J. Performance optimization of the endoreversible simple MCBC coupled to variable-temperature reservoirs based on NSGA-II Algorithm. *Power Gener. Technol.* **2020**, in press (In Chinese).

60. Tang, C.Q.; Feng, H.J.; Chen, L.G.; Wang, W.H. Power density analysis and multi-objective optimization for a modified endoreversible simple closed Brayton cycle with one isothermal heating process. *Energy Rep.* **2020**, *6*, in press.
61. Arora, R.; Kaushik, S.C.; Kumar, R.; Arora, R. Soft computing based multi-objective optimization of Brayton cycle power plant with isothermal heat addition using evolutionary algorithm and decision making. *Appl. Soft Comput.* **2016**, *46*, 267–283.
62. Qi, W.; Wang, W.H.; Chen, L.G. Power and efficiency performance analyses for a closed endoreversible binary Brayton cycle with two isothermal processes. *Therm. Sci. Eng. Prog.* **2018**, *7*, 131–137.
63. Chen, L.G.; Zheng, J.L.; Sun, F.R.; Wu, C. Performance comparison of an irreversible closed variable-temperature heat reservoir Brayton cycle under maximum power density and maximum power conditions. *Proc. IMechE Part A J. Power Energy* **2005**, *219*, 559–566.
64. Chen, L.G.; Zheng, J.L.; Sun, F.R.; Wu, C. Performance comparison of an endoreversible closed variable temperature heat reservoir Brayton cycle under maximum power density and maximum power conditions. *Energy Convers. Manag.* **2002**, *43*, 33–43.
65. Cheng, C.Y.; Chen, C.K. Ecological optimization of an endoreversible Brayton cycle. *Energy Convers. Manag.* **1998**, *39*, 33–34.
66. Zheng, J.L.; Chen, L.G.; Sun, F.R. Power density analysis of an endoreversible closed Brayton cycle. *Int. J. Ambient Energy* **2001**, *22*, 95–104.